ELSEVIER

Marine and Petroleum Geology 15 (1998) 593–617

Marine and Petroleum Geology

The source rock horizons of the Ionian Basin (NW Greece)

N. Rigakis[a,*], V. Karakitsios[b]

[a] *Hellenic Petroleum S.A. Exploration and Production Division, 199, Kifissias Ave. 15124 Maroussi, Athens, Greece*
[b] *Department of Geology, National University of Athens, Panepistimioupoli, 15784 Athens, Greece*

Received 27 February 1998; revised 18 May 1998; accepted 28 May 1998

Abstract

The organic geochemical study of six geological sections and two wells in the Ionian Zone (NW Greece), allows us to distinguish five horizons of possible source rocks: The Vigla shales (Cenomanian–Turonian), the Upper Posidonia Beds (Callovian–Tithonian), the Lower Posidonia Beds (Toarcian–Aalenian), the marls at the base of the Ammonitico Rosso (Early Toarcian), and shale fragments incorporated within the Triassic breccias. These horizons have good hydrocarbon potential and an organic matter type I to II.

In the deeper parts of the Botsara sub-basin, the oil window is located in the interval between 3700–5800 m depth. Consequently, the Triassic shales have already entered the gas window. The Lower and Upper Posidonia Beds, and the marls at the base of the Ammonitico Rosso are mature in terms of oil generation. The Vigla shales maturity corresponds to the early maturation stage. The timing of the principal oil-source horizons maturation is the Late Jurassic for the Triassic shale beds and the Serravalian for the Lower Posidonia Beds.

The preservation of the organic matter in the Lower and Upper Posidonia Beds through Toarcian to Tithonian and in the marls at the base of the Ammonitico Rosso during Early Toarcian are directly related to the geometry of the syn-rift period of the Ionian Basin. The organic matter preservation in the Vigla shales is related to the sub-basins that were preserved by the continuation of halokinetic movements during the post-rift period. The geometry of the restricted sub-basins that were formed during the syn-rift and post-rift period of the Ionian Basin evolution favored water stagnation and the development of local euxinic conditions in the bottom waters; these conditions were accentuated during the anoxic events that are known to have affected the Tethys ocean during the Early Toarcian and Late Cenomanian. The organic rich shale fragments within the Triassic breccias were initially deposited as stratigraphic layers in sub-basins of the evaporitic basin. The establishment of evaporitic sedimentation in the entire basin favored the preservation of the organic matter. The processes that resulted in the formation of the evaporite dissolution collapse breccias caused also the fragmentation of the organic rich layers, which are present actually as organic rich shale fragments within the Triassic breccias.

Keywords: Source rocks; Ionian Basin; Western Greece; Oil window; Depositional model

1. Introduction

The surface occurrences of petroleum in the Ionian Zone of northwestern Greece are mainly attributed to the Toarcian Lower Posidonia Beds and to a lesser extent to the Late Callovian-Tithonian Upper Posidonia Beds and the Albian-Cenomanian Upper Siliceous Zone or 'Vigla Shales' of the Vigla Limestones (IGRS-IFP, 1966; Nikolaou, 1986; Baudin and Lachkar, 1990; Roussos and Marnelis, 1995; Karakitsios, 1995; Karakitsios and Rigakis, 1996).

Oil that cannot be attributed to the above source rocks is believed to originate from Triassic formations that contain potential source rocks in Albania and Italy (Roussos and Marnelis, 1995). Indeed, in a preliminary work we have identified some beds containing shale fragments rich in organic matter, in between the Triassic breccias of northwestern Greece (Karakitsios and Rigakis, 1996).

In this work, we will present our analytical results of 6 geological sections and two wells (Dragopsa-1 and Ioannina-1 wells), where, except for the already known oil source rocks of the Ionian Zone, we identified two new oil-source rocks: the marl beds at the base of the Ammonitico Rosso and some horizons containing oil-source shale fragments in the Triassic breccias.

2. Geological frame

The Ionian Zone of northwestern Greece (Epirus region) constitutes part of the most external zones of the

* Corresponding author. Tel.: 0030 1 806 9301; fax: 0300 1 806 9317.

S0264–8172/98/$—see front matter
PII: S0264–8172(98)00032–4

Hellenides (Paxos Zone, Ionian Zone, Gavrovo Zone; Fig. 1a). The rocks of the Ionian Zone range from Triassic evaporites and associated breccias through a varied series of Jurassic to Upper Eocene carbonates and, to a lesser degree, cherts and shales followed by Oligocene flysch (Fig. 2).

In the Early Liassic, northwestern Greece was covered by a huge carbonate platform (Bernoulli and Renz, 1970; Karakitsios, 1992). In the Pliensbachian, extensional stresses associated with the opening of the Tethys Ocean caused the opening of the Ionian Basin (Bernoulli and Renz, 1970; Karakitsios, 1990; 1992). Even though the production of platform carbonates persisted through the entire Jurassic in the adjacent Paxos (pre-Apulian) and Gavrovo Zones, the Ionian Basin became an area of stronger faulting and ensuing subsidence. This paleogeographic configuration continued with minor off-and onlap movements along the basin margins until the late Eocene when orogenic movements and flysch sedimentation began. In the Gavrovo and Ionian Zones, the main orogenic movements took place at the end of the Burdigalian, while in the Paxos and Apulian Zones they occurred during the Pliocene–Pleistocene (IGRS-IFP, 1966; Bizon, 1967).

Analysis of the Ionian Basin allows us to distinguish three distinct sequences (Karakitsios, 1995) (Fig. 2):

The pre-rift sequence which is represented by the Early Liassic Pantokrator Limestones (Aubouin, 1959; IGRS-IFP, 1966; Karakitsios, 1990; 1992). These shallow water limestones overlie Early to Middle Triassic evaporites (more than 3000 m thick) through the Foustapidima Limestones of Ladinian-Rhetian age (Renz, 1955; Pomoni-Papaioannou and Tsaila-Monopolis, 1983; Dragastan et al., 1985; Karakitsios and Tsaila-Monopolis, 1990). The 'sub-evaporite beds' of the Ionian Zone in Western Greece do not crop out, nor were they penetrated by wells (IGRS-IFP, 1966; BP, 1971).

The syn-rift sequence began with the deposition of the Siniais Limestones and their lateral equivalent, the Louros Limestones (Karakitsios and Tsaila-Monopolis, 1988). Foraminifera, brachiopods and ammonites in the Louros Limestones indicate a Pliensbachian age (Karakitsios, 1990; 1992). These formations correspond to the general subsidence of the area (formation of the Ionian Basin), which was followed by the internal syn-rift differentiation of the Ionian Basin marked by smaller paleogeographic units. These paleogeographic units are recorded in the prismatic synsedimentary wedges of the syn-rift formations and include the Siniais or Louros Limestones (Pliensbachian), the Ammonitico Rosso or Lower Posidonia Beds (Toarcian–Aalenian), the 'Limestones with Filaments' (Bajocian–Callovian), and the Upper Posidonia Beds (Late Callovian–Tithonian) (Karakitsios et al., 1988; Karakitsios, 1995; Fig. 2). Stratigraphic sections measured throughout the study area display abruptly changing thicknesses of the syntectonic sequences within a few kilometers. The opening of the Tethys Ocean was accompanied by the formation of a series of north-northwest- and east-southeast -trending conjugate faults. The early Liassic shallow marine platform was affected by listric block-faulting, which was recorded in the differential subsidence within each small paleogeographic unit (Bernoulli and Renz, 1970; Karakitsios, 1992). The directions of synsedimentary tectonic features (e.g., slumps and synsedimentary faults) indicate that deposition was controlled by structures formed during the extensional tectonic phase. The sedimentation style corresponds, in general, to a half-graben geometry. Prismatic synsedimentary wedges of the syn-rift formations in the small paleogeographic units (in most cases the units did not exceed 5 km across) vary in thickness east-west. Thus, unconformities are located on top of tilted blocks and complete Toarcian to Tithonian successions with Ammonitico Rosso or Lower Posidonia Beds at their base are located in the deeper parts of the half grabens. Theoretical considerations and field data suggest that the extensional phase provoked halokinesis in the Ionian Zone evaporitic substratum; the halokinesis influenced the syn-rift mechanism by increasing the extensional fault throws (Karakitsios, 1988; 1990; 1992; 1995).

The post-rift period was defined by an early Berriasian breakup that is marked by an unconformity at the base of the Vigla Limestones. Sedimentation during the post-rift period was synchronous in the whole Ionian Basin (Karakitsios, 1990; Karakitsios and Koletti, 1992). The post-rift sequence (Vigla Limestones and overlying Alpine formations) largely obscures the syn-rift structures and in some cases, overlies directly the pre-rift sequence (Karakitsios, 1992; 1995). The deposits of the Vigla Limestones do not correspond to an eustatic sea-level rise, but to a general sinking of the entire basin (Karakitsios and Koletti, 1992). The permanence of differential subsidence during the deposition of the Vigla Limestones, shown by the strong variation in thickness of this formation, is probably due to the continuation of halokinetic movements of the Ionian Zone evaporitic substratum (IGRS-IFP, 1966; Karakitsios, 1988; 1990; 1992).

Observation of the Ionian Zone tectonics shows that structures (folds and thrusts) in the central and western parts of the Ionian Zone are displaced westwards, whereas in its eastern part they are displaced eastwards (Fig. 1b). The Ionian Zone constitutes a good example of inversion tectonics in a basin with an evaporitic substratum (Karakitsios, 1995). Balanced cross-sections constructed through an intermediate and a more external part of the basin show that, several times during the compressional phase, faults related to the extensional phase did not reactivate as thrusts, as the classical scheme of inversion tectonics suggest; in contrast, due to evaporitic substratum halokinesis, the most elevated footwalls have been thrust over the pre-existing hanging walls

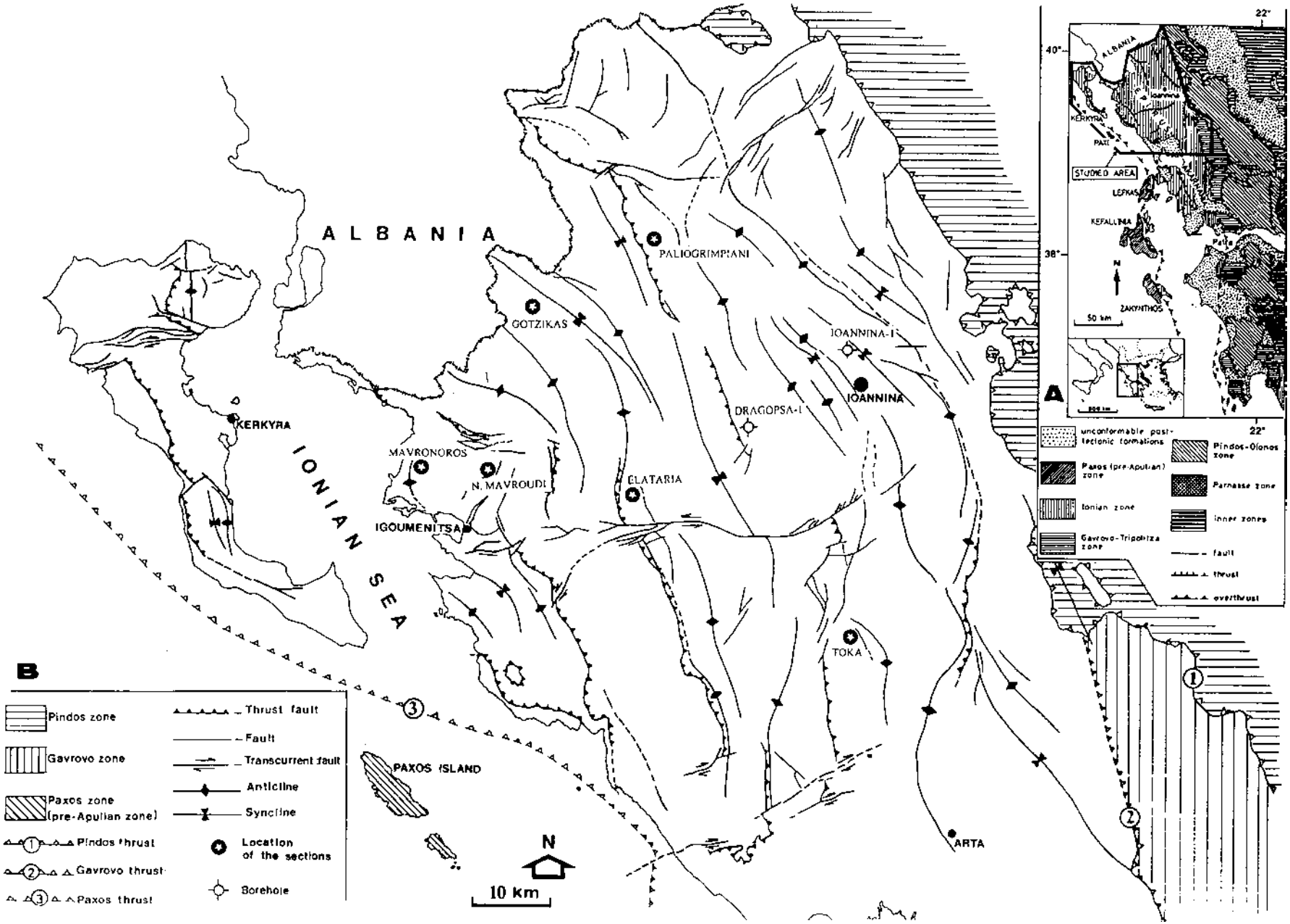

Fig. 1. (a) Structural map of the western continental Greece (after Karakitsios, 1995). (b) Structural map of the Epirus region (after Karakitsios, 1995) and locations of the geological sections and boreholes.

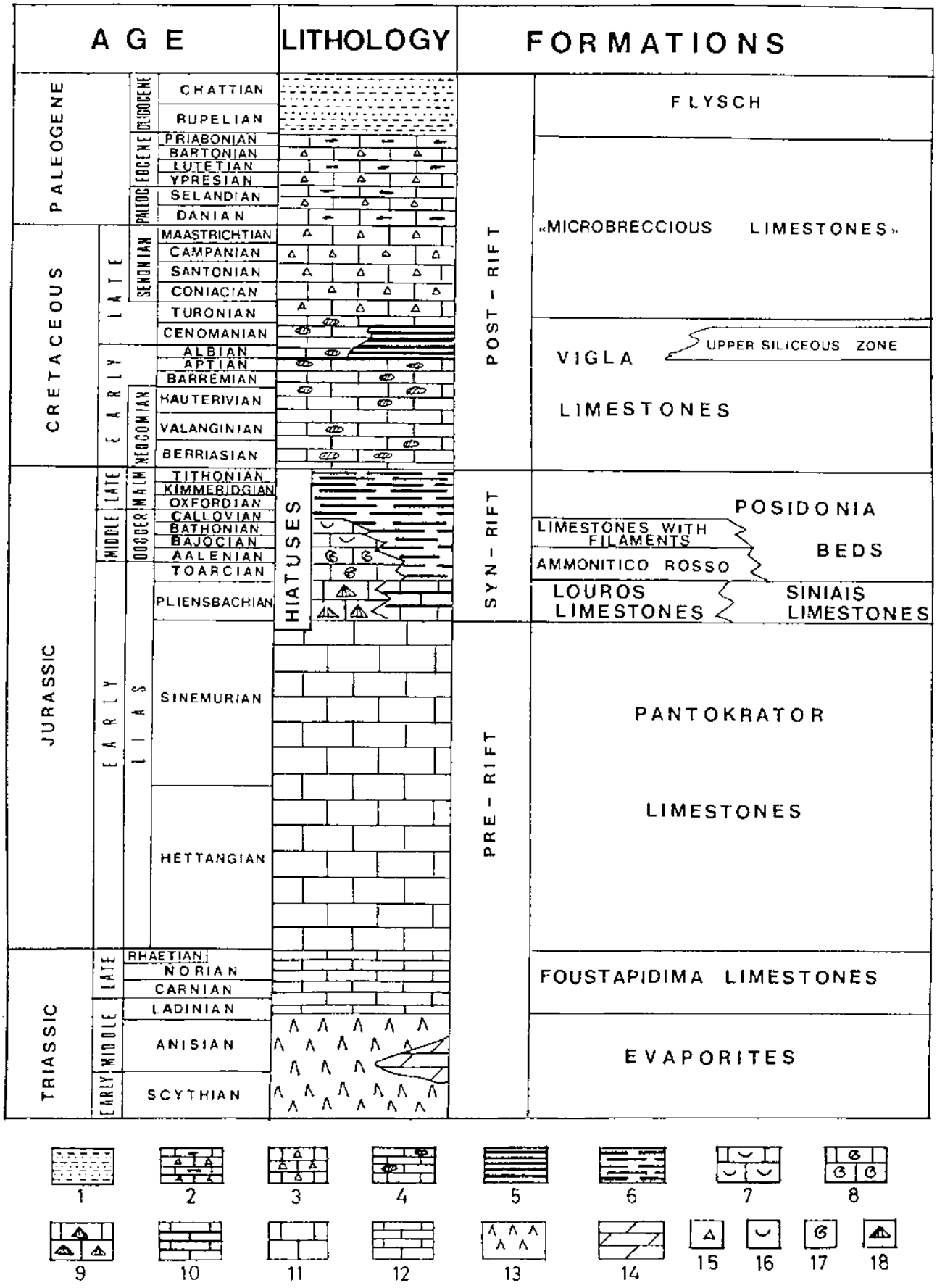
AGE
LITHOLOGY
FORMATIONS
PALEOGENE
OLIGOCENE
EOCENE
PALEOC.
CHATTIAN
RUPELIAN
PRIABONIAN
BARTONIAN
LUTETIAN
YPRESIAN
SELANDIAN
DANIAN
FLYSCH
«MICROBRECCIOUS LIMESTONES»
CRETACEOUS
LATE
SENONIAN
MAASTRICHTIAN
CAMPANIAN
SANTONIAN
CONIACIAN
TURONIAN
CENOMANIAN
EARLY
ALBIAN
APTIAN
BARREMIAN
NEOCOMIAN
HAUTERIVIAN
VALANGINIAN
BERRIASIAN
POST - RIFT
VIGLA
UPPER SILICEOUS ZONE
LIMESTONES
JURASSIC
LATE
MALM
TITHONIAN
KIMMERIDGIAN
OXFORDIAN
MIDDLE
DOGGER
CALLOVIAN
BATHONIAN
BAJOCIAN
AALENIAN
EARLY
LIAS
TOARCIAN
PLIENSBACHIAN
HIATUSES
SYN - RIFT
POSIDONIA
LIMESTONES WITH FILAMENTS
BEDS
AMMONITICO ROSSO
LOUROS LIMESTONES
SINIAIS LIMESTONES
SINEMURIAN
HETTANGIAN
PRE - RIFT
PANTOKRATOR
LIMESTONES
TRIASSIC
LATE
RHAETIAN
NORIAN
CARNIAN
LADINIAN
MIDDLE
ANISIAN
EARLY
SCYTHIAN
FOUSTAPIDIMA LIMESTONES
EVAPORITES
1
2
3
4
5
6
7
8
9
10
11
12
13
14
15
16
17
18

(Karakitsios, 1995). The amount of shortening involves a westward increase of horizontal displacement of the Ionian Zone. Since the estimation of the shortening was only based on surface geological data, it should be regarded as conservative (Karakitsios, 1995). However, in all cases the occurrence of reverse faults and thrusts took place in the location of Jurassic paleofaults (Karakitsios. 1995). The double divergence of the Ionian structure (westward in the western and central parts and eastward in the eastern part, respectively) is attributed to the structures inherited from the extensional Jurassic phase (Karakitsios, 1995). The extensional Jurassic faults of the external Ionian Zone (Apulian side) dipping eastwards, were reactivated during the compressional phase as compressional westward displacements, whereas those of the internal Ionian Zone (Gavrovo side) dipping westwards, were reactivated as compressional eastward displacements. Listric faults were transformed entirely into transcurrent faults, or reverse faults and/or thrusts, which is consistent with the classical inversion tectonics. Where halokinesis played an important role in the development of the structures, the reverse fault movement occurred only in the upper parts of the faults. This phenomenon was facilitated by diapiric movements of the evaporitic base through the above mentioned tectonic surfaces. Field data and available seismic lines point out that a moderate decollement zone developed in the sub-surface evaporites, especially in the external domain of the Ionian Zone (Karakitsios, 1995).

3. Possible hydrocarbon source rocks of the Ionian sequence

There are five main horizons within the carbonate series of the Ionian Zone that could generate significant amounts of hydrocarbons

(1) The 'Vigla Shales' member of the Vigla Limestones formation, which correspond to the Upper Siliceous zone of IGRS-IFP (1966). This member is consisted of limestone and cherty beds with dark gray to green or red shale interbedding. The 'Vigla Shales' were dated in detail to Albian-Cenomanian interval (IGRS-IFP, 1966). The above stratigraphic member is examined in the Gotzikas section and in the Ioannina-1 well (Figs. 1b and 3).

The Gotzikas section is located in a valley, near Tsamantas village. The stratigraphic sequence starting from flysch includes the Eocene Limestones, the Senonian Limestones and the Vigla Limestones formation (the only one with geochemical interest). The outcropping thickness of the Vigla Limestones is about 180 m, while the expected formation thickness in this area is 600 m (IGRS-IFP, 1966). The Vigla Limestones consist of thin-bedded gray packstones in rhythmical alternations with chert layers and intercalations of shale horizons. The two first shale horizons are found at 80 m from the formation top (Fig. 3). These horizons are very thin (5−7 cm thick) with very low carbonate content ($CaCO_3 = 6\%$) and very low density. In the limestones of the next 90 m interval, there are two shale horizons, consisting of very thin-bedded marly limestones, followed, in the next 13 m of the section, by the most significant shale horizons (Fig. 3). These horizons include 15 shale layers, some of which pinch-out stratigraphically. Each horizon is 15–30 cm thick, and their total thickness is 3 m. It is unknown whether these shale horizons continue in the subsurface. Samples were taken from all the lithographical horizons: the bituminous shales, the shale horizons and the gray packstones.

In the Ioannina-1 well the Vigla formation is the first Alpine formation underlying the Quaternary and Neogene sediments. It covers the interval between 300–610 m depth (Karakitsios, 1995). Some shaly horizons, corresponding to the 'Vigla shales' member, were found from 460–480 m depth.

(2) The Upper Posidonia Beds. This formation is consisted of yellow to green jasper beds (5–10 cm thick) with cherty clays, often bituminous. The cherty horizons are rich in Posidonia (*Bositra*) and Radiolaria of the Late Callovian to Tithonian (Karakitsios et al., 1988). The formation is studied in the Mavronoros section (10 km NNW of Igoumenitsa) (Figs 1b and 3). In this area the well developed Ammonitico Rosso (reddish nodular limestones and marls rich in Ammonite fauna) does not contain at its base significant marl horizons. It is overlain by some meters of Limestones with Filaments, followed by the Upper Posidonia Beds. The latter are represented by the typical facies of thin-bedded siliceous argillites and cherts containing abundant pelagic bivalves and radiolaria. In the lower part thin intercalations of mostly chertified lumachelles with large planktonic bivalves ('*Posidonia*' = *Bositra*), to which the formation owns its name, are present. The total thickness of the formation is about 9 m.

In many places of the Ionian Zone, the Upper

←

Fig. 2. Representative stratigraphic column of the Ionian Zone (after Karakitsios, 1995): 1 = pelites and sandstones; 2 = cherty limestones with clastic material; 4 = pelagic cherty limestones; 5 = cherty beds with green and red clay, sometimes shaly; 6 = pelagic limestones, marls, and siliceous argillites; 7 = pelagic limestones with pelagic bivalves; 8 = pelagic, red, nodular limestones with ammonites; 9 = micritic limestones with small ammonites and brachiopods; 10 = pelagic limestones; 11 = platform limestones; 12 = platy black limestones; 13 = gypsum and salt; 14 = dolomites; 15 = breccia; 16 = section of pelagic bivalve (filament); 17 = ammonite; 18 = brachiopod.

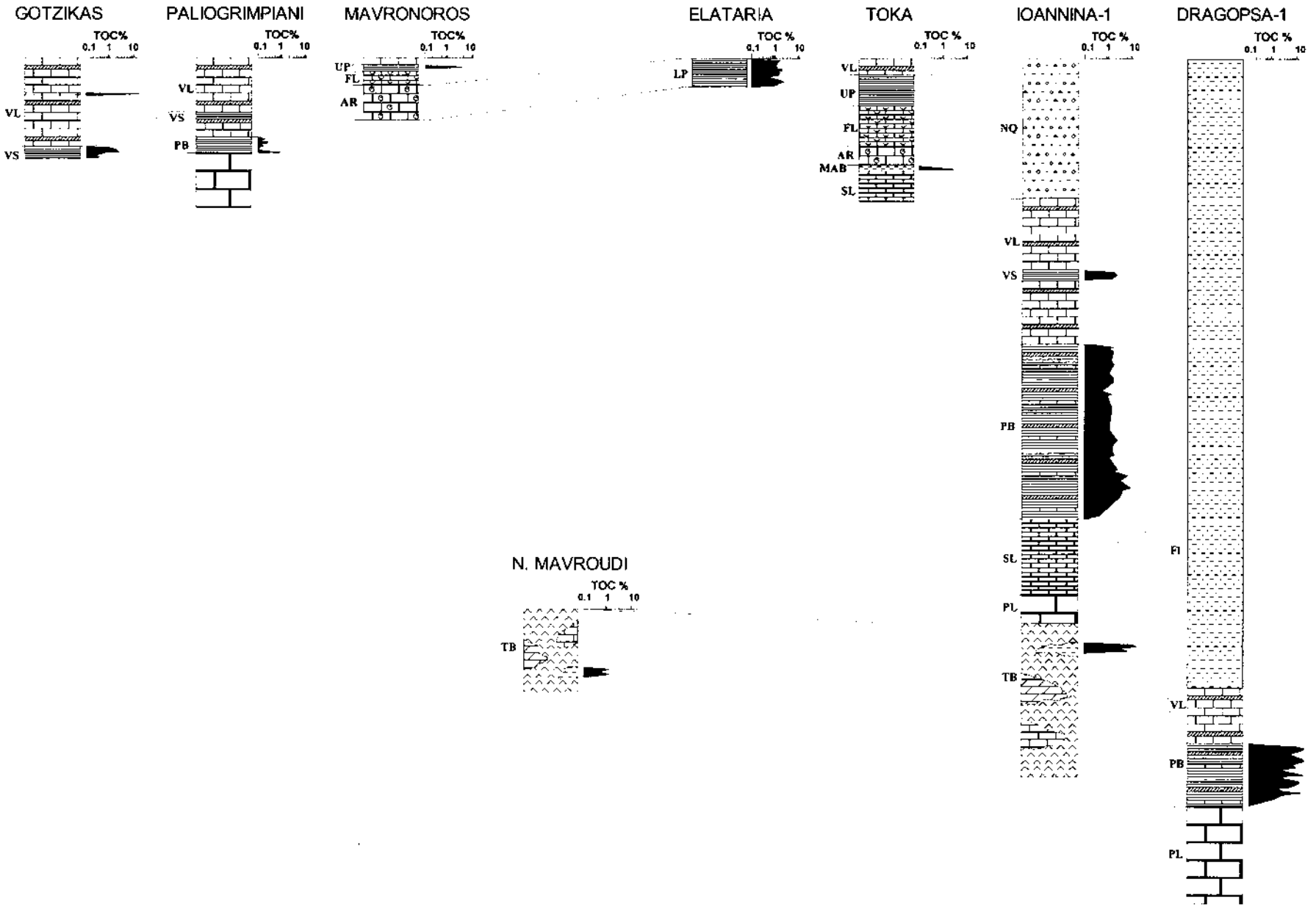

Fig. 3. Selected lithological sections and wells and vertical distribution of organic matter in the Ionian Zone, Epirus (location of the sections and wells in Fig. 1): NQ, quaternary and Neogene; FL, Flysch; VL, Vigla Limestones; VS, Vigla Shales; UP, Upper Posidonia Beds; FL, Limestones with filaments; LP, Lower Posidonia Beds; AR, Ammonitico Rosso; MAB, Marls at the base of AR; PB, undifferentiated Posidonia Beds; SL, Siniais Limestones; PL, Pantolcrator Limestones; TB, Triassic breccias.

Posidonia Beds are not clearly differentiated form the Lower Posidonia Beds, so the whole formation is examined as 'undifferentiated Posidonia Beds' (e.g., Paliogrimpiani section, and Dragopsa-1 and Ioannina-1 wells; Figs 1b and 3).

(3) The Lower Posidonia Beds. This formation is composed of well-bedded pelagic limestones, marles, and siliceous argillites and show variations in facies and thickness (IGRS-IFP, 1966; Walzebuck, 1982) depending on their position in each half graben (Karakitsios, 1990; 1992). IGRS-IFP (1966) deduced the age of the Toarcian formation from the stratigraphic frame, and recent studies on nannofossil assemblages support that age (Baldanza and Mattioli, 1992). This formation constitutes the main source rock horizon of the Ionian Zone (Jenkyns, 1988; Baudin and Lachkar, 1990; Karakitsios, 1995; Roussos and Marnelis, 1995; Karakitsios and Rigakis, 1996). It is found in many places and contains high amounts of organic matter. The formation is examined in the Elataria and Paliogrimpiani sections and the Ioannina-1 and Dragopsa-1 wells (Figs 1b and 3).

Elataria section, is located in the Paramithia mountains, north of the Petoussi transcurrent fault (Fig. 1b), In this area, the Lower and Upper Posidonia Beds are separated by some meters of the Limestones with Filaments formation, and the total thickness of the succession is 150 m. The Lower Posidonia Beds correspond to the first 41 m of the succession. They consist of green to gray marly limestones ($CaCO_3 = 57–65\%$) intercalated with thin-bedded dark gray marls ($CaCO_3 = 30–45\%$), and some slightly siliceous lumachelles rich in radiolaria and large pelagic bivalves (*Bositra*). The formation top is dominated by black cherty layers. Coniferous branches were found in the marls at the formation base (Karakitsios, 1992; 1995). Samples were taken mainly from the marls and the marly limestones.

In the Paliogrimpiani section, in the eastern part of Kassidiaris mountain, the undifferentiated Posidonia Beds were observed. In this area, the whole stratigraphic sequence of the Ionian Zone appears, from the Triassic breccias and evaporites (found in the Parakalamos plain), up to the latest Alpine sediments of flysch. The undifferentiated Posidonia Beds begin with 20 cm of a relatively cohesive gray marly horizon, followed by weathered and very loose, cream, thin-bedded marly limestones, siliceous argillites and cherts (more affected by the weathering are the very thin-bedded horizons).

In the Ioannina-1 well the undifferentiated Posidonia Beds cover the interval from 610–990 m depth. They are represented by alternations of marly limestones, black shales and cherts. A direct measurement of dip in the alternating limestone and marl in the core sample at 960 m depth gave a dip of 45°; so the real formation thickness might be lower than the drilled thickness corresponding to this formation.

Dragopsa-1 well penetrated the undifferentiated Posidonia Beds in the depth interval of 1477.5–1601 m. The lithological members of the formation are siliceous marly limestones in alternations with very thin-bedded marls and thin layers of chert. The interval of 1547–1556 m as well as the formation base consist of light cream limestones. The formation interval containing marly horizons is 100 m thick (Fig. 3). Taking into account that dip ranges from 36–50°, as measured in the core samples at 1450–1485 m depth respectively, the real formation thickness is estimated to be less than 80 m. Samples were analyzed from every shaly horizon. In particular, the thin-bedded marls were hand-picked and analyzed separately.

(4) The marls underlying the Ammonitico Rosso Limestones. They are consisted of dark gray to blue-green foliated marls and marly, slightly siliceous lime wackestones. This lithological member is observed only in the areas where the Ammonitico Rosso of Toarcian-Aalenian age (Renz, 1955; Aubouin, 1959; Karakitsios, 1990) is well developed. These areas correspond to the depocenters of the half grabens created by the Ionian Basin internal syn-rift differentiation (Karakitsios, 1995).

The marls at the base of the Ammonitico Rosso were studied in the Toka section, 1.5 km northwest of Ano Kouklessi village (Figs 1b and 3). From the 30 m of total thickness of the Ammonitico Rosso formation in this section, 10 m correspond to the above mentioned lithological member, consisting of blue-green to gray marls in alternations with marly nodular limestones.

(5) The Triassic shale fragments. They constitute parts of the Triassic breccias which correspond to typical evaporite dissolution collapse breccias (Karakitsios and Pomoni-Papaioannou, 1988). The Triassic breccias have been dated by the discovery of Early-Middle Triassic Foraminifera in dolomites intercalated into gypsum deposits (Pomoni-Papaioannou and Tsaila-Monopolis, 1983; Dragastan et al., 1985). It has been proved that the organic matter of the shale fragments in the Triassic breccias cannot be originated from the already known source rocks of Ionian Zone (e.g., Posidonia beds), but they represent a new source rock horizon (Karakitsios and Rigakis, 1996). They were studied in the North Mavroudi section and Ioannina-1 well (Figs 1b and 3).

In North Mavroudi, black shale fragments were identified within the breccias of Triassic age. Similar shale fragments were found in the Ioannina-1 well, at a depth interval from 1250–1275 m.

All the above formations vary in thickness and extent in the Ionian Basin, as well as in their organic

matter content. These variations, as shown in the next chapters, depend on the paleogeographic position and the depositional environment.

4. Analytical methods

The analytical procedures of this study follow common practices, frequently used in petroleum geochemistry. Well samples, mainly cuttings, were obtained every 2–5 m interval, especially from the formations with geochemical interest. After washing and removal of contaminants, samples were dried at 50°C and pulverized. For petroleum potential determination the Rock-Eval method (Espitalie et al., 1977) was used: As quantity parameters were used the total organic carbon (TOC%) and the petroleum potential (PP mg/g), which is determined as the sum of S1 (free hydrocarbons) and S2 (kerogen) peaks. The type of organic matter was determined by the combination of hydrogen index (HI = S2/TOC) and oxygen index (OI = S3/TOC) in a pseudo van Krevelen diagram (Tissot and Welte, 1984), as well as from the S2/S3 ratio (Peters, 1986). Furthermore, samples were selected from every horizon of interest and investigated microscopically under transmitted and reflected light (Teichmuller, 1986). The principal maceral groups were identified and additional information were obtained about the kerogen quality. As maturity parameters were used the T_{max} and the production index ($PI = S1/S2+S2$) from the Rock-Eval method, as well as, the spore coloration expressed by the thermal alteration index (TAI) and the vitrinite reflectance (Ro %), from the optical examination of the organic matter. Further information on the organic matter characteristics were obtained by chemical analyses of bitumens of the potential source rocks. So we selected one sample from each horizon and performed the following procedures (Palacas et al., 1984): Extraction by soxhlet with chloroform, fraction separation by column chromatography, gas chromatography (GC) of the $C_{15}+$saturated HC, Gas chromatography–mass spectroscopy (GCMS) of saturated and aromatic HC fractions. For the last analysis we used some biomarker classes, such as steranes, terpanes and aromatic steroids as maturity parameters.

5. Hydrocarbon potential

The hydrocarbon potential evaluation, which has been performed separately for each individual formation, has as follows:

5.1. Vigla formation

The Vigla Shale horizons in the Gotzikas section are rich in total organic carbon (TOC = 0.94–2.54%) and have a high petroleum potential (PP = 4.85–11.69 mg HC/g of rock; Fig. 4a and Appendix). Their organic matter is of type II (Fig. 5a), with main components being amorphous matter, algae and exinite (Table 1). The pr/ph ratio is between 1.81–2.54, confirming the marine environment of deposition of their organic matter (Powell, 1986; Mello et al., 1988; Peters and Moldowan, 1993). The S2/S3 ratio is higher than 5, indicating that the organic matter is oil prone (Peters, 1986). So these horizons, having a good potential of type II organic matter, can generate significant quantities of oil. Especially the first two horizons in the Gotzikas section are very rich in organic carbon (TOC = 19.1–21.6%) and petroleum potential (PP = 178.6–182.6 mg/g). Furthermore, their hydrocarbon content is extremely high (HC = 32140 ppm). Their very low OI in combination with the very high HI indicate a type I organic matter. The microscopical examination of the kerogen shows 99–100% amorphous and algal matter. All the examined parameters indicate very good quality of their organic matter and characterize these horizons highly oil-prone source rocks. The analytical results and physical properties classify the above horizons to typical bituminous shales (Tissot and Welte, 1984), the only one known in Greece.

The shales of the Vigla Formation in the Ioannina-1 well have a good potential of generating hydrocarbons, since their TOC values are greater than 1% (Peters, 1986; Bordenave et al., 1993). TOC of the Vigla Shales ranges from 1.44–2.24% (Figs 4a, 6 and Appendix). Petroleum potential ranges from 7.3–13.6 mg HC/g of rock, indicating the presence of a good source rock potential. The HI values are greater than 475 and up to 600 in some instances, (Fig. 6 and Appendix) thus indicating good quality of the organic matter. These HI values are plotted vs OI in the diagram of Fig. 5a. From this plot, which is similar to the van Krevelen diagram (Tissot and Welte, 1984), we conclude that the kerogen of the Vigla shales is of type I to II, originated from marine organisms (phytoplankton, zooplankton and bacteria) in a reducing environment and is capable of generating mainly liquid hydrocarbons. This result is supported by the visual examination of the kerogen concentrates. The percentage of algal and amorphous material ranges from 57 to almost 100% (Table 1). These macerals indicate the presence of type I–II organic matter (Tissot and Welte, 1984; Teichmuller, 1986; Bertrand et al., 1993).

5.2. Upper Posidonia beds

Two horizons of the Upper Posidonia beds in the Mavronoros section gave positive results, in terms of oil generation. Their richness in organic matter (TOC = 2.51–3.47%, Fig. 4b and Appendix) and the organic matter of type II (Fig. 5b) associated with them are both conclusive of their oil generation potential.

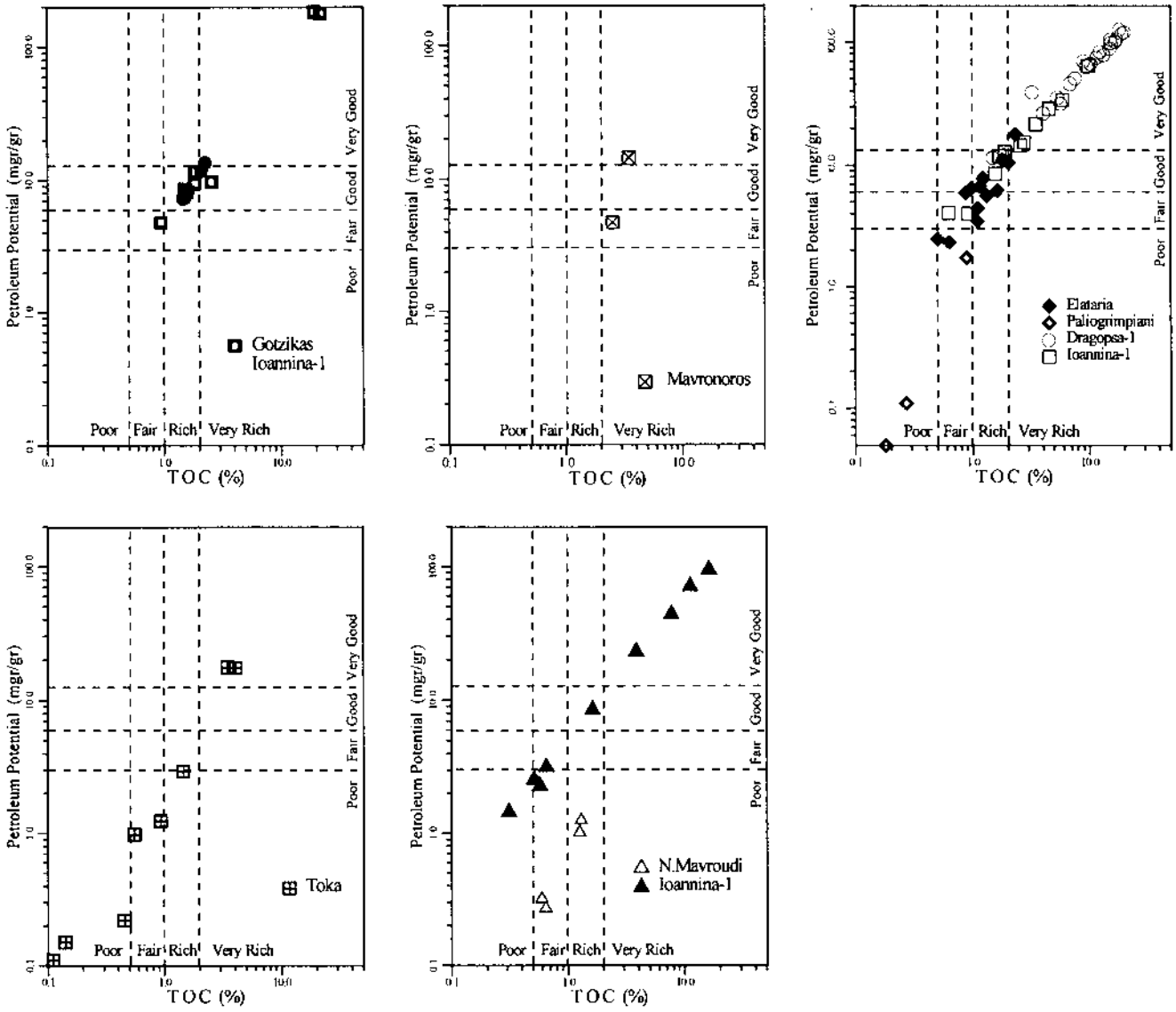

Fig. 4. TOC vs petroleum potential indicating the occurrence of rich source rocks in the formations: (a) Vigla Limestones; (b) Upper Posidonia Beds; (c) Lower Posidonia Beds; (d) Marls at the base of Ammonitico Rosso; (e) Triassic shales.

5.3. *Lower Posidonia beds*

In the Elataria section, all the measured samples are characterized by a high quantity of organic matter, since their TOC ranges from 1.10–3.02% and their petroleum potential from 4.43–17.84 mg HC/g of rock (Fig. 4c and Appendix). The organic matter is of type II (Fig. 5c) and the S2/S3 ratio is greater than 5. The isoprenoid indicators confirm the Rock-Eval quality indexes and only the visual kerogen examination shows a significant amount of vitrinite, coming from organic matter of terrigenous origin. In fact, in the same area coniferous branches were observed in the base of Lower Posidonia Beds, involving terrestrial drifts that can be explained if the depositional environment was close to an emerged area favorable to coniferous life (Karakitsios, 1992; 1995). Generally these source rocks can generate remarkable quantities of oil. On the other hand, in the Paliogrimpiani section only the first horizon of the formation contains remarkable quantities of organic matter, having a TOC of 0.88% (Fig. 4c and Appendix), close to the lower limit of a rich source rock, and a type II organic matter (Fig. 5c), capable for oil generation. All the other horizons showed negligible quantities of organic matter.

The undifferentiated Posidonia Beds in the Ioannina-1 well have a good oil generation potential. Rock-Eval data from these horizons, as well as of all the formations penetrated by the Ioannina-1 well, are plotted in Fig. 6. In the same diagram the gamma ray log is also plotted for the same well: it is known from worldwide experience that the gamma ray increases in the intervals with high TOC, due to the enrichment of organic matter in uranium

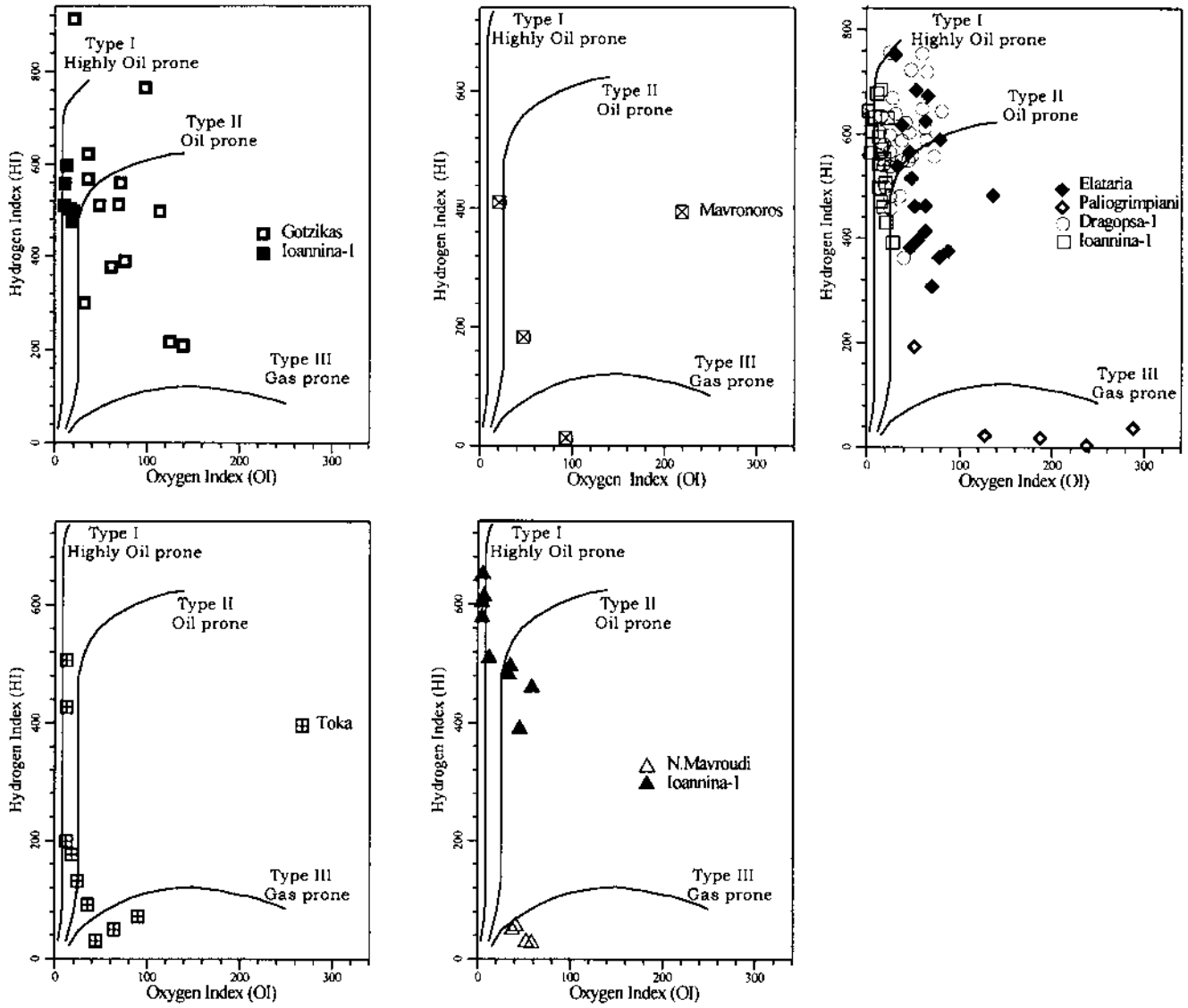

Fig. 5. HI vs OI plot showing the hydrocarbon generation types. The examined samples from all the possible source rocks consist of type I to II organic matter. (a) Vigla Limestones; (b) Upper Posidonia Beds; (c) Lower Posidonia Beds; (d) Marls at the base of Ammonitico Rosso; (e) Triassic shales.

(Schmoker, 1981; Fertl, 1983). In the Ioannina-1 well the results are not always comparable. The first increase in the gamma ray values is observed in the Vigla shales at the interval of 460–480 m. After that the gamma ray decreases in the remaining part of the Vigla horizons, while an increase appears again in the Posidonia Beds interval. This increase does not correspond to a high TOC, especially in the interval of 900–980 m. Following that, high gamma ray values show up in between 1050–1070 m depth without any increase in the organic matter content, as well as in the interval of 1250–1270 m, where the Triassic potential source rocks have been identified. Finally, high gamma ray values are observed in the deepest part of the Ioannina-1 well (1370–1500 m) that do not correspond with high TOC values. All these high gamma ray values, in the intervals with low TOC, are due to the presence of radioactive minerals not associated with organic facies deposition. This type of mineral has been found in the Mitsikeli mountain, a few km east of the Ioannina-1 well (Koukouzas et al., 1978).

The TOC of the Posidonia Beds ranges from 1.05–4.50% (average 1.75%), with two extreme values of 5.87% and 9.82% at 910 m and 940 m respectively (Figs 4c, 6 and Appendix). Petroleum potential ranges from 4.00–21.54 mg HC/g of rock (average 9.2), with three extreme values at 945, 910 and 940 m depth of 28.90, 33.88 and 64.09 mg HC/g of rock respectively. Both quantity parameters indicate a good source rock potential. The HI values range from 460–565, indicating the good quality of the organic matter (Fig. 6 and Appendix). The

Table 1
Kerogen composition and maturity measurements by microscopical examination of kerogen concentrates. Am = amorphus material; Al = algal; Res = resinite; Vitr = vitrinite; Iner = inertinite; TAI = thermal alteration index; Ro = vitrinite reflectance; a, b, c = vitrinite populations with different reflectivity measurements; ND = not determined.

	Sample data			Kerogen concentrates (%)				Maturity indicators (Ro%)			
Area/well	No.	Depth (m)	Formation	Al+Am	Res	Vitr.	Iner.	a	b	c	TAI
Gotzikas	1403	0	Vigla	99	—	1	—	0.44			1.0
Gotzikas	1413	0	Vigla	80	5	15	—	0.50			2.5
Elataria	927	0	Posidonia	40	—	60	—	0.31			1+/2
Elataria	932	0	Posidonia	40	—	60	—	0.58			1+/2
Elataria	936	0	Posidonia	50	—	50	—	0.31			1+/2
Elataria	941	0	Posidonia	30	—	70	—	0.64			1+/2
Elataria	946	0	Posidonia	50	—	50	—	0.31			1+/2
Mavronoros	2407	0	Posidonia	33	65	1	1	0.44	0.64		ND
Ioannina-1		480	Vigla	65	2	5	28	0.62			1+
Ioannina-1		625	Posidonia	73	2	5	20	0.79			1+
Ioannina-1		690	Posidonia	72	3	5	20	0.38	0.62	0.84	1+
Ioannina-1		800	Posidonia	57	1	9	33	0.42	0.67	0.96	1+
Ioannina-1		945	Posidonia	78	1	1	20	0.55	0.75		1+
Ioannina-1		964	Posidonia	68	—	1	33	0.39	0.61	1.01	1+
Ioannina-1		1185	Pantokrator	99	—	—	1	0.38			ND
Ioannina-1		1250	Triassic	99	—	—	1	0.30	1.41		1+/2
Dragopsa-1	210	0	Flysch	—	—	80	20	0.41			2+
Dragopsa-1	209	0	Flysch	—	—	60	40	0.45			2+
Dragopsa-1	207	0	Flysch	—	—	60	40	0.44			2+
Dragopsa-1		777	Flysch	—	—	—	—	0.47			ND
Dragopsa-1		1485	Posidonia	ND	ND	ND	ND	0.51			ND
Dragopsa-1		1486	Posidonia	90	—	10	—	0.54			ND
Dragopsa-1		1530	Posidonia	90	—	10	—	0.60			2+
N.Mavroudi	284	0	Triassic	70	—	30	—	1.01			1.5

latter correlate with the low OI values in the pseudo van Krevelen diagram of Fig. 5c, indicating that the type of organic matter is I–II, prone to oil generation. Similar results derive from the microscopical examination of eight samples from this formation (Table 1). The percentage of algal and amorphous material that indicate the presence of type I–II organic matter, ranges from 57–78%. This percentage may be even higher; the examined samples were cuttings and were analyzed without removing the inert portion which possibly increases the concentration of inertinite (Table 1).

In the Dragopsa-1 well, the horizons of the siliceous marly limestones, lithological member of the Posidonia Beds, are rich in organic carbon (TOC = 1.10–5.88%) and have a high petroleum potential (PP = 5.91–39.46 mg/g, Figs 4c, 7). Their organic matter is of type I–II, as deduced by the correlation of the high HI and the low OI (Fig. 5c) as well as the high quantities of algal matter contained in the kerogen concentrates (Table 1). Even higher quantities of organic matter are included within the thin-bedded marls, with TOC between 6.85–19.12% and petroleum potential between 46.00–125.85 mg/g, with the algal matter being the main kerogen compound. These horizons are the best known source rocks in Western Greece.

5.4. Marls at the base of the Ammonitico Rosso

Most of the horizons contain low quantities of organic matter, but there were identified two horizons with very high organic matter content (Fig. 4d and Appendix). Their organic matter content ranges between 3.46–4.07% and their petroleum potential is also high, reaching up to 17.6 mg/g. The organic matter of these two horizons is of type I, highly oil prone (Fig. 5d). Most of the other horizons have a type II organic matter and only in a few horizons is significant terrigenous input identified, as inferred by their organic matter of type III.

5.5. Triassic breccias

In the N. Mavroudi section, two shale fragments rich in organic carbon (TOC = 1.25–1.29%), but poor in petroleum potential (PP = 0.26–1.46 mg HC/g of rock; Fig. 4e and Appendix) were found. This difference between TOC and PP can be a result of:

(1) The presence of coal. In this case these horizons can not be characterized as oil-prone source rocks.
(2) The presence of residual carbon. In this case the initial content in organic carbon was significantly higher

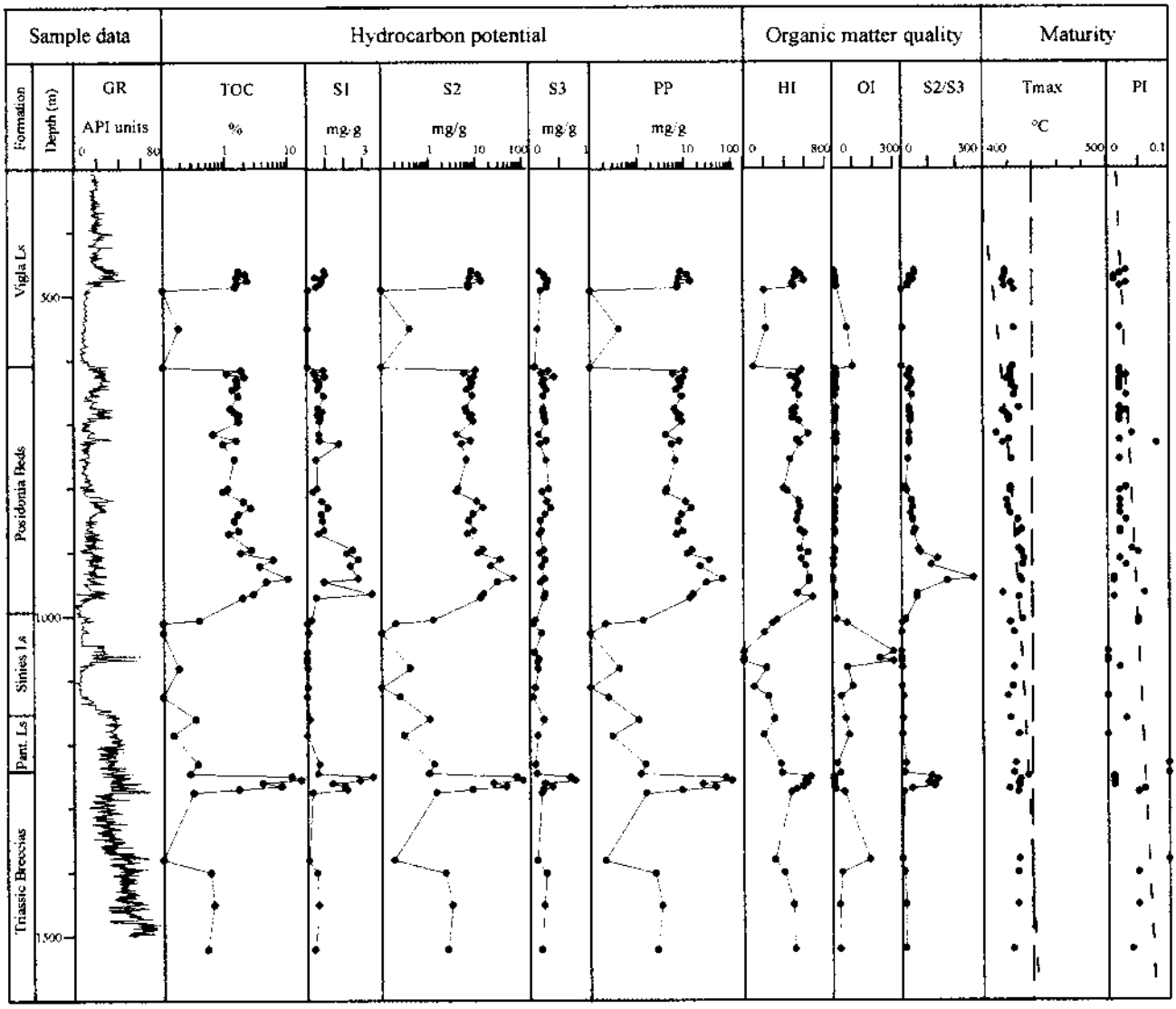

Fig. 6. Geochemical profile of Ioannina-1 well. Ls: Limestones; Pant. Ls: Pantokrator limestones; GR: Gamma Ray; TOC: Total organic carbon; S1: Free hydrocarbons; S2: Pyrolysable hydrocarbons; S3: CO_2 from pyrolysis; PP: Petroleum potential (S1 + S2); HI: Hydrogen Index (S2 × 100/TOC); Oxygen Index (S3 × 100/TOC); T_{max}: Temperature of the top of S2 peak; PI: Production Index (S1/S1 + S2).

and should correspond to an equally high value of petroleum potential. However, the high maturity of the organic matter brought about a decrease in the whole oil potential and consequently the remaining petroleum potential is very low. At the same time the enrichment in carbon has resulted in a relatively high residual TOC value of the source rock. This is also supported by the quality indicators that appear to decrease due to the high maturity.

In the Ioannina-1 well the analyses of some shale fragments from the Triassic breccias gave very high amounts of organic matter (Karakitsios and Rigakis, 1996). First a pure shale fragment was analysed from a core at 1250 mm depth, indicating a very high TOC up to 11.15% (see Appendix). The corresponding petroleum potential value was also extremely high, reaching 74.02 mg HC/g of rock. The organic matter of this sample is also of very good quality (type I, Fig. 5e). This organic matter consists of algal and amorphous matter in a proportion of 99% (Table 1). In addition to this sample some more shale fragments were identified in the interval of 1250–1270 m with very high TOC (1.62–16.12%), very good petroleum potential (8.9–98.8 mg HC/g of rock) and type I oil-prone organic matter (Figs 4e, 5e).

6. Maturity

Several parameters have been examined for estimating the thermal maturity of the potential source rocks. The maturity of the outcrop samples is generally low since these horizons have been emerged prior to the maturation of their organic matter. More reliable measurements have

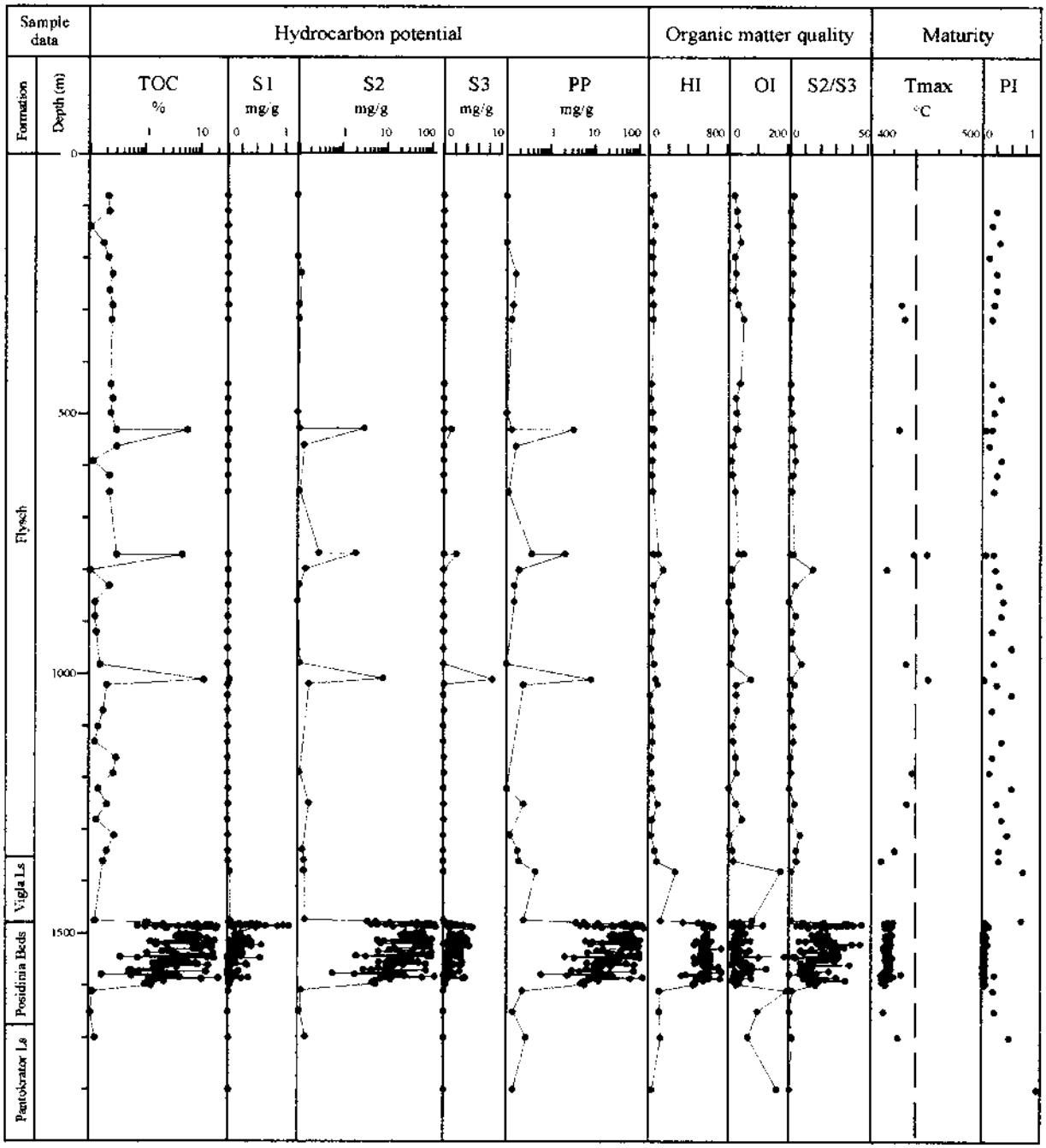

Fig. 7. Geochemical profile of Dragopsa-1 well. For identification of parameters see Fig. 6.

been effected in well samples. These wells were drilled on top of tilted blocks forming the sub-basins where the formations pinch-out; so, the measured maturity is not representative of the maturation degree of the sediments deposited at the basin depocenters.

Three of the parameters obtained from the Rock–Eval pyrolysis were examined as maturity indicators: Maximum pyrolysis temperature-T_{max}, production index-PI and hydrogen index-HI. Each of these parameters indicates the immaturity of the organic matter. The T_{max} of the outcrop samples is generally lower than 435°C, the upper limit of oil window (Espitalie et al., 1977; Peters, 1986) and the PI is lower than 0.1. Only in the Triassic samples the T_{max} and the PI gave high values, indicating that the organic matter has entered the oil window. Low maturity characterizes also the organic matter of the well samples. In the Ioannina-1 well the T_{max} values are less than 435°C and only the sample at 1250 m depth has a T_{max} value of 436°C, corresponding to the top of the oil window. Furthermore, the trend in the diagram T_{max}–

depth (Fig. 6) indicate an increase of T_{max} with depth. According to that, the upper limit of the oil window is estimated to be at about 1400 m depth. In the Dragopsa-1 well, the T_{max} is less than 435°C in all the formations and the trend in the diagram T_{max}–depth (Fig. 7) does not indicate clearly an increase of T_{max} with depth in order to predict the upper limit of the oil window. PI values in the well samples are too low, indicating first immaturity and second absence of any migrated hydrocarbons. HI values are generally too high, indicating immaturity of the organic matter. For a graphical prediction of the maturity we used the diagrams of Fig. 8, which are cross-plots of T_{max} vs HI for each well. These diagrams clearly indicate that the organic matter for all the formations has a predicted vitrinite reflectance (Ro) value of less than 0.5%, so their organic matter is immature for oil generation. On the other hand, the good quality of the organic matter (type I or II) is confirmed again.

The vitrinite reflectance-Ro values of most of the outcrop samples are lower than 0.60% (Table 1), showing that the present-day surface organic matter has not entered the main oil generation phase. One horizon of the Posidonia Beds in the Elataria section has an Ro value of 0.64%, but most of the other samples in this section are immature (0.31% Ro). Finally, the most mature of the outcrop samples is included within the north Mavroudi Triassic shales, it is in the oil window having an Ro equal to 1.01 and it is close to the maximum of oil generation. These Triassic sediments were buried at significant depths for a long period to the orogenesis,

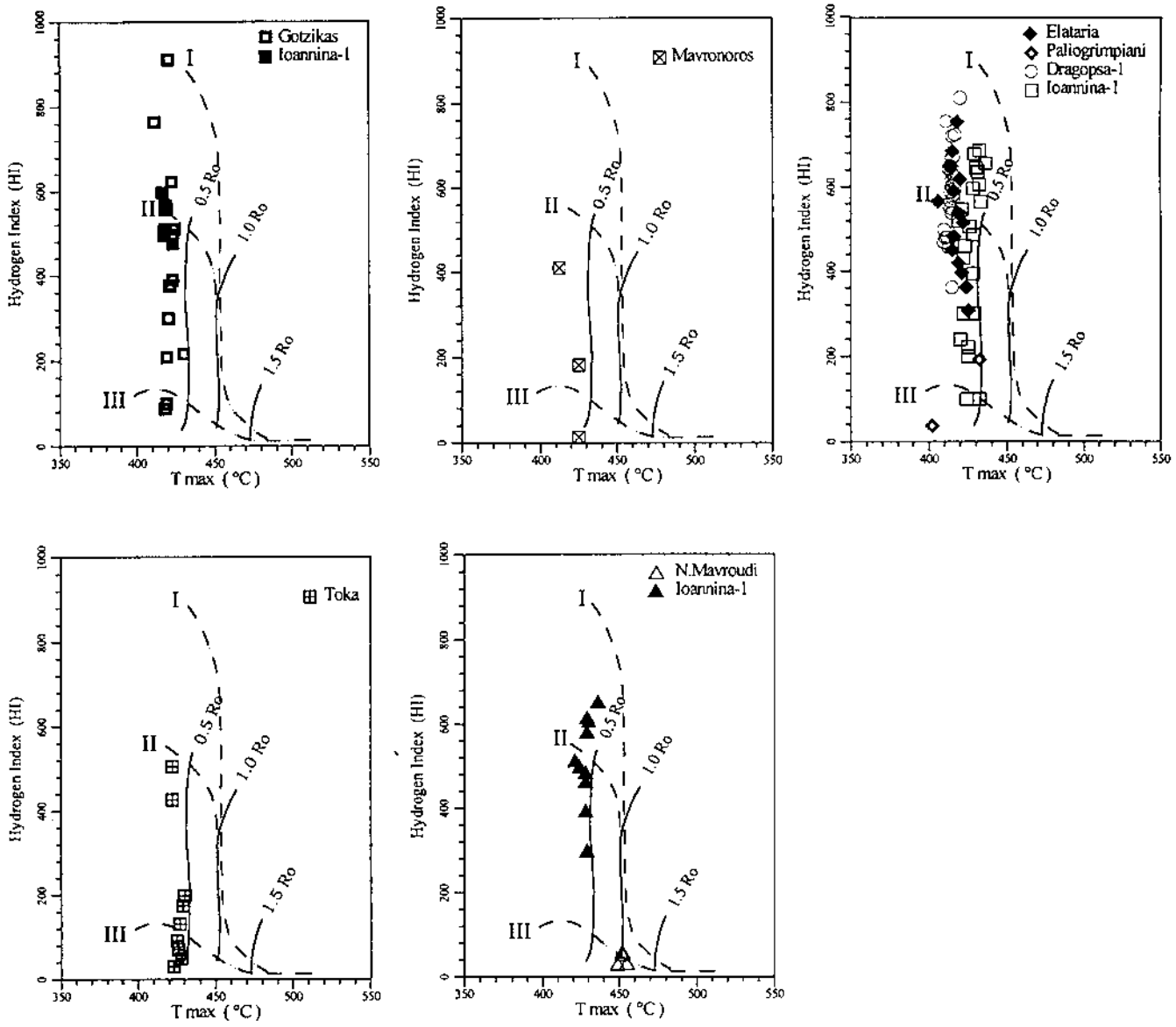

Fig. 8. HI vs T_{max} plot showing the organic matter maturity. Samples are immature, but close to the onset of oil generation. (a) Vigla Limestones; (b) Upper Posidonia Beds; (c) Lower Posidonia Beds; (d) Marls at the base of Ammonitico Rosso; (e) Triassic shales.

so their organic matter was affected by a high degree of maturation. In the examined source rocks of the Ioannina-1 well, the vitrinite reflectance values are inconsistent, probably due to very low participation of the vitrinite maceral in the kerogen of these rocks. This actually happens in organic matter type I and II (Tissot, 1984) where vitrinite is rare. The concentration of vitrinite type macerals in the eight examined samples ranges from traces up to 9% (Table 1). On the other hand, the percentage of inertinite type macerals is significantly higher, ranging from 1–33%. Based on this, we consider that many of the reflectance measurements derive from inertinite type macerals. Actually, in most of the samples two or three different populations of reflecting macerals have been identified (Table 1). The second and third population are considered typical of inertinite. Reworked material, increasing the reflectance values, is contained even within the first population of most samples. Consequently the values of the first population are not considered to be representative of the organic matter maturity. Indeed, the plot of these values in a diagram vs depth indicates a negative maturity trend (Fig. 9), which is inconsistent with the geological framework of the area. It is thus concluded that the vitrinite reflectance measurements are probably unreliable for the prediction of the thermal maturity in the Ioannina-1 well. In the Dragopsa-1 well there is one measurement from a core sample at 777 m depth within the flysch, with an Ro = 0.47% and three more within the Posidonia Beds, the first at 1481 m depth with an Ro = 0.51%, the second at 1486 m depth, with an Ro = 0.54% and the third at 1530 m depth, with an Ro = 0.60%. These measurements are combined with those corresponding to surface samples from the area in the vicinity of the well (derived from three flysch horizons) whose Ro values are 0.41%, 0.44% and 0.45% (Table 1). The surface maturity measurements plotted with those of the well samples result in a curve showing a normal maturity increase with depth (Fig. 10). By extrapolation of this curve we conclude that the main oil generation in the Dragopsa-1 well starts at a depth of 1880 m.

The spore coloration, as expressed by the thermal alteration index—TAI, is expected to be more reliable than the vitrinite reflectance in our case due to the organic matter type. However, the measured values of TAI are very low, indicating the immaturity of the organic matter. In the Ioannina-1 well for example, the values of TAI are 1+ for all the samples (Table 1), apart from the sample

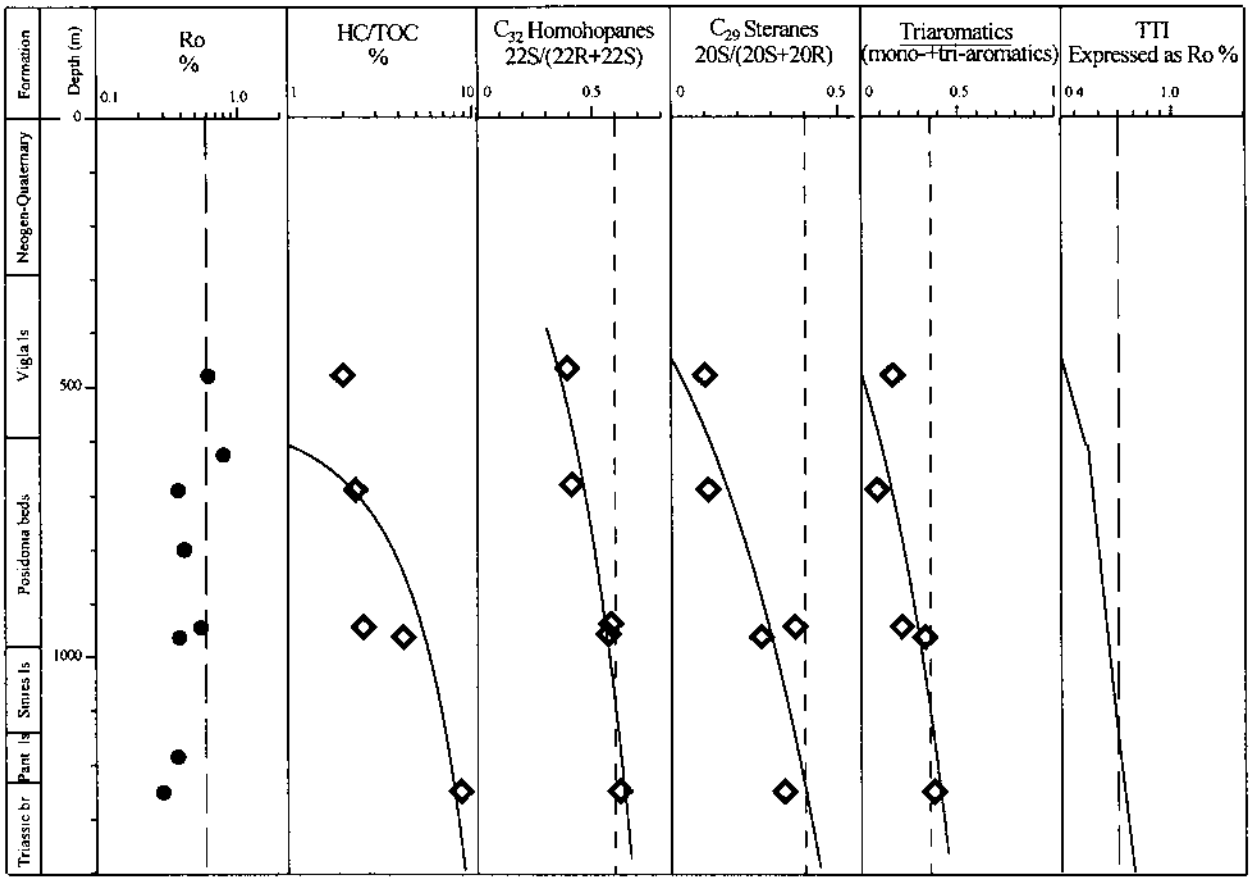

Fig. 9. Maturity diagrams vs depth, Ioannina-1 well. For identification of biomarker indicators see Table 2; Ro = vitrinite reflectance %; TTI = time temperature index.

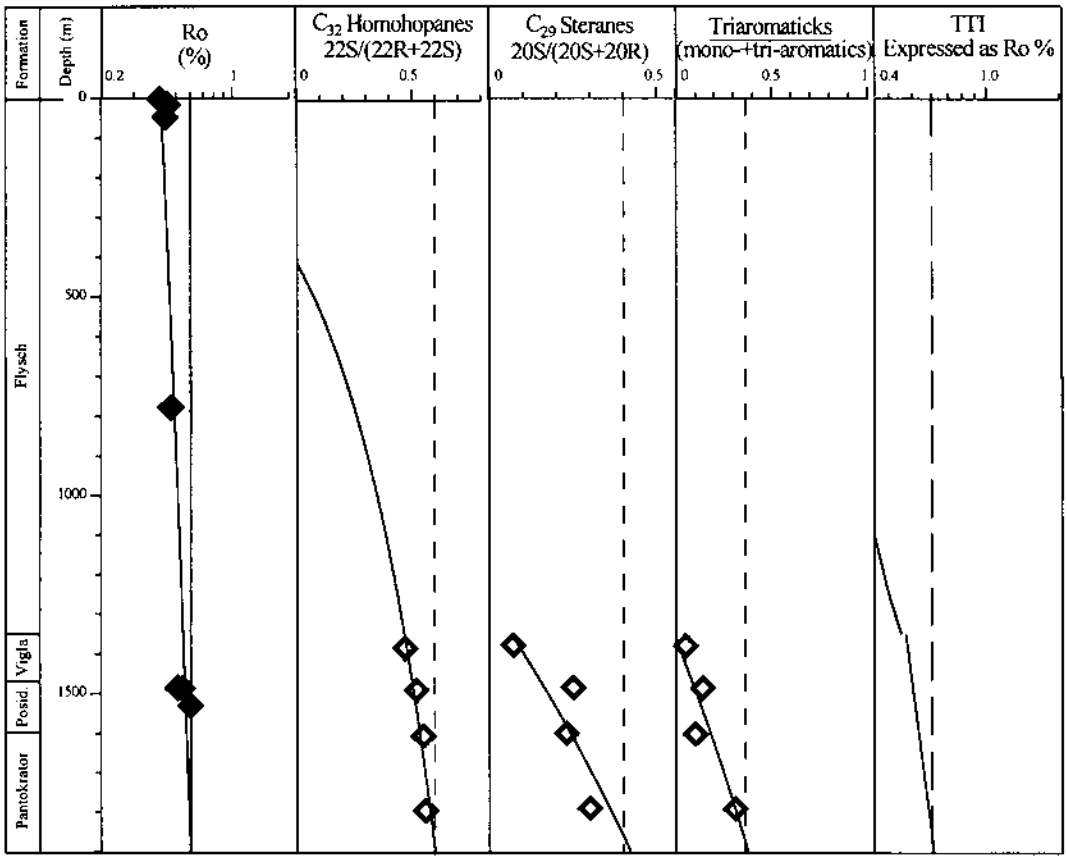

Fig. 10. Maturity diagrams vs depth, Dragopsa-1 well. For identification of biomarker indicators see Table 2; Ro = vitrinite reflectance %, TTI = time temperature index.

at 1185 m depth that was impossible to measure, due to inclusions of atypical-unrecognizable matter or interstitial bitumen. The measured values of 1+ characterize the organic matter of the sediments as immature on the basis of oil generation potential (Teichmuller, 1986; Bertrand et al., 1993).

From the biomarker maturity parameters we examined the ratios of C_{32} homohopanes, C_{29} steranes and the aromatic/steroid ratio (Table 2). The 22S/(22R+22R) ratio of C_{32} 17a(H) homohopanes is very sensitive to low maturity ranges. The equilibrium value of this ratio is 0.60 (Mackenzie, 1984; Peters and Moldowan, 1993), corresponding to the onset of oil generation. This value is reached at 1880 m depth in the Dragopsa-1 well and 1100 m depth in the Ioannina-1 well. These depth are fairly well correlated with the calculated depths by other methods. The 20S/(20R+20S) ratio of C_{29}5a(H), 14a(H) and 17a(H) steranes can be used as maturation level indicators up to a range of 0.8% Ro (Mackenzie, 1984; Peters and Moldowan, 1993). In the studied area, this ratio displays an increase with well depth. In the Dragopsa-1 well this increase is correlated with the Ro vs depth curve, as well as the C_{32} homohopanes 22S/(22R+22R) vs depth curve (Fig. 10). From this correlation the upper limit for oil generation was defined at the 20S/(20R+20S) ratio value of 0.40 of the C_{29} steranes. By using these data in the Ioannina-1 well it is expected that the oil window will be at 1250 m depth, very close to the calculated depth from the other methods. From the aromatic steroids we used the triaromatic/(triaromatic+monoaromatic) steroid ratio which has given very satisfactory results in western Greece (Palacas et al., 1986; Palacas et al., 1989). In this ratio, as 'triaromatic' are used the compounds $C_{20}+C_{28}$ triaromatic steroids and as 'monoaromatic' is taken the C_{29} monoaromatic steroid (Palacas et al., 1986). The well-section measurements of this ratio gave comparable results to those of the other methods (Figs. 9, 10). The onset of oil generation, based on the aromatic steroids, is at 1880 m depth in the Dragopsa-1 well and 1100 m depth in the Ioannina-1 well. These depths are also well correlated with the calculated maturity by using the time-temperature history of these wells (Waples, 1980). The time-temperature index (TTI), expressed as vitrinite reflectance (Ro) values, is plotted next to the biomarker ratio in the diagrams of Figs 9 and 10. From these diagrams, it is inferred that the onset of oil generation, as calculated from the TTI method, occurs at a depth similar to that found from the biomarker maturity indicators.

In the Ioannina-1 well the biomarker maturity par-

Table 2
Extraction–hydrocarbon separation data and biomarker ratios characteristic of the possible source rocks' maturity. EOM = extractable organic matter; HC = hydrocarbons; TOC = total organic carbon; Sat = saturate hydrocarbons; pr = pristane; ph = phytane; C_{32}Terp = 17a(H) C_{32} homohopane 22S/(22S+22R); C_{29} = [5a(H), 14a(H), 17a(H)], C_{29} regular sterane 20S/(20S+20R); T = C_{20}+C_{28} triaromatic steroids; M = C_{29} monoaromatic steroid; ND = not determined.

Area/well	Sample	Depth	EOM	HC		Satur.	HC/TOC	C_{32}Terp	C_{29}Ster	T/T+M
	No.	(m)	(ppm)	(ppm)	(%)	pr/ph				
Gotzikas	1403	0	25228	8826	35	1.81	3.08	0.56	0.25	0.23
Gotzikas	1413	0	4578	2310	50	2.07	8.95	0.58	0.26	0.17
Elataria	928	0	242	148	61	1.78	1.10	ND	ND	ND
Elataria	938	0	281	138	49	1.28	0.80	ND	ND	ND
Elataria	947	0	325	127	39	1.19	0.50	ND	ND	ND
Ioannina-1		480	272	60	21	1.44	1.97	0.39	0.10	0.16
Ioannina-1		690	673	206	31	1.74	2.31	0.41	0.11	0.08
Ioannina-1		945	3056	266	9	0.65	2.55	0.58	0.37	0.21
Ioannina-1		964	4068	907	22	1.42	4.20	0.57	0.27	0.33
Ioannina-1		1250	11554	1494	13	0.48	8.68	0.62	0.34	0.38
Dragopsa-1		1380	803	ND	ND	ND	ND	0.47	0.07	0.05
Dragopsa-1		1485	2143	1034	48	1.40	5.78	0.52	0.25	0.14
Dragopsa-1		1600	224	91	41	0.87	3.03	0.55	0.23	0.10
Dragopsa-1		1790	40	ND	ND	ND	ND	0.58	0.30	0.31

ameters were also combined with the ratio of the hydrocarbons extracted from the source rocks to the total organic carbon (HC/TOC). This ratio is continuously increasing with depth (Fig. 9), thus indicating that the maximum of oil generation is deeper than the well total depth (Claypool et al., 1978).

For maturity predictions in the deeper horizons of the Ionian Zone we drew some more burial history curves in order to calculate the time-temperature index (TTI, Waples, 1980). One of those, in the deepest part of the Botsara sub-basin, is shown in Fig. 11. The thickness of the various formations is: Burdigalian 1500 m, flysch 1500 m, Eocene to Senonian Limestones 600 m, Vigla Limestones 700 m, undifferentiated Posidonia Beds 200 m, Pantokrator and Siniais Limestones 2000 m, Foustapidima Limestones 200 m, Triassic evaporites-breccia > 3000 m. For the thermal data we proceeded as follows: The present day geothermal gradient is 2.05°C/100 m for the clastics and 1.74°C/100 m for the carbonates. The paleogradient, starting from Triassic with the value of 'continental' type sediments (2.5°C/100 m), rises in combination with the progressive thinning of the marginal continental crust, up to a maximum of 3.5°C/100 m until the end of deposition of the Vigla Limestones. After that, the gradient starts to decrease first to an initial value in the Early Oligocene and finally up to its present value. All these data are compatible with the temperature and maturity measurements in the deep wells of western Greece.

From the burial history curves, the following are inferred about the five source rock horizons: The Triassic sediments have passed through the oil window and have already entered the gas window. The base of the Ammonitico Rosso and the Lower and Upper Posidonia Beds have entered the oil window. The Vigla shales are in the early mature stage. Furthermore, from the diagram of TTI vs. depth (Fig. 12), we conclude that the upper limit of the oil window is at a depth of 3700 m, the lower limit at 5800 m depth and the lower limit of gas window at 6900 m depth. The TTI of the main source rock, the Lower Posidonia Beds, is 29 and corresponds to an Ro of 0.78%, close to the maximum of oil generation. Finally from the burial history curve and especially from the diagram of TTI vs. time (Fig. 13) the relative maturity dating can be accomplished. So the oldest source rock horizons, the Triassic source rocks, have entered the oil window in the Late Jurassic (140 Ma), while the main source rock horizon, the Lower Posidonia Beds, at Serravallian time (15 Ma), after the main orogenetic phase.

7. Depositional model

Except for the shale fragments which are incorporated within the Triassic breccias, the conditions of source rock deposition as well as organic matter preservation for the remaining of the source rocks are in general the same. More specifically:

The accumulation and preservation of the organic matter in the Lower and Upper Posidonia Beds through Toarcian to Tithonian and in the marls at the base of the Ammonitico Rosso during Early Toarcian, are directly related to the geometry of the syn-rift period of the Ionian Basin. The geometry of the restricted sub-basins favored water stagnation and consequently the development of locally euxinic conditions in the bottom waters (Karak-

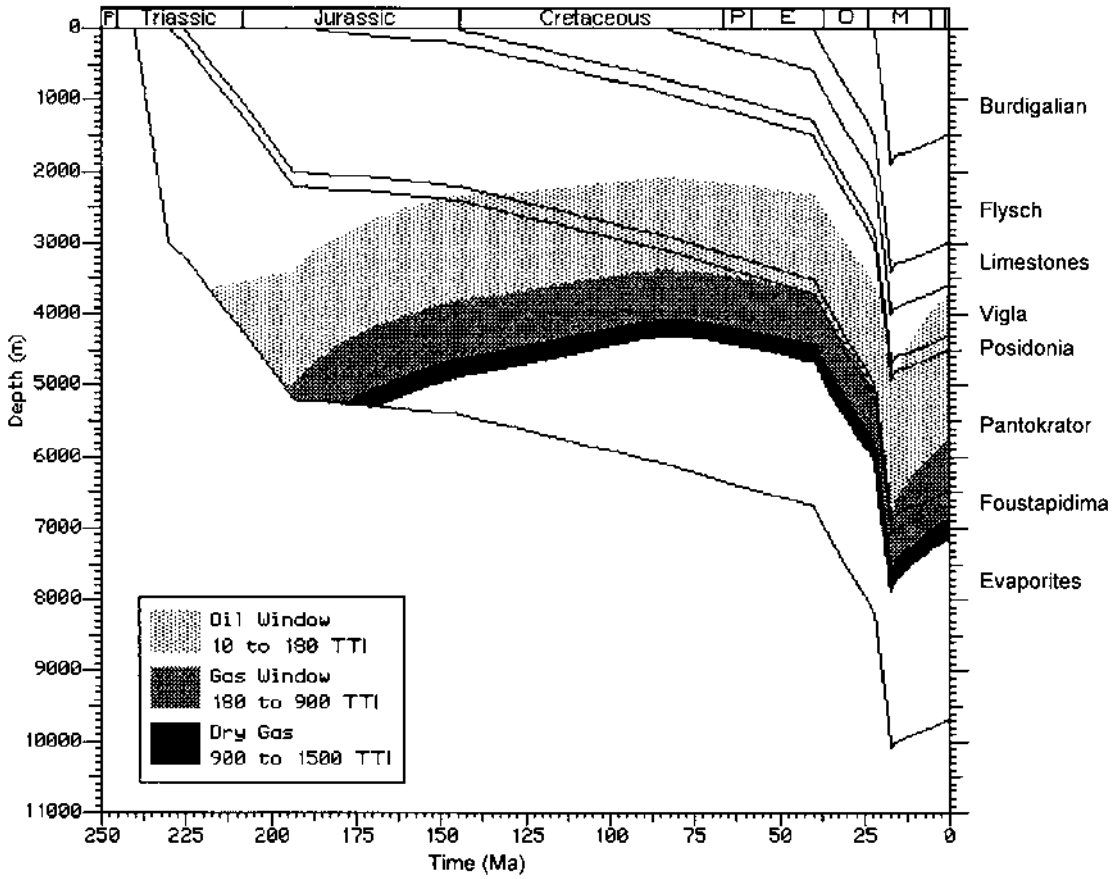

Fig. 11. Burial history diagram in the deepest part of Botsara sub-basin.

itsios, 1995). Anoxic conditions occurred locally even during the post-rift period in the areas where the Vigla shales lithological member (Albian–Cenomanian) of the Vigla Limestones is well developed; these areas probably represent sub-basins that were preserved due to the continuation of halokinetic movements during the post-rift period (Karakitsios, 1995). The well documented Toarcian (Jenkyns, 1988; Farrimond et al., 1989) and Cenomanian/Turonian (Farrimond et al., 1990) oceanic anoxic events that affected the entire Tethys ocean, influenced the preservation of organic matter in Ionian Zone. Thus, the particular geometry of the sub-basins during the syn-rift and post-rift period of the Ionian Zone favored the record of both anoxic events, as it is shown by the high amount of organic matter included in the Lower Posidonia beds (Toarcian) and the Vigla Shales (Albian-Cenomanian).

The dimensions of the source rock horizons corresponding to the Lower Posidonia Beds is a significant problem. High amounts of organic matter were deposited and preserved in the depocenters of the half grabens, while this amount was reduced towards the shallower areas. This aspect is strengthened by the fact that, in the Parliogrimbiani section and other areas as well, only the deepest shale horizon contains significant amounts of organic matter. This horizon was deposited in an anoxic environment which changed to more oxic (with the progressive filling of the graben) in the upper horizons of the formation. Evidently the Ioannina-1 and Dragopsa-1 wells were drilled in areas corresponding to the deepest parts of the half-grabens that account for the entire high thickness of the sedimentary strata as well as the source rock richness.

The Triassic breccias of the Ionian Zone correspond to typical evaporite dissolution collapse breccias (Karakitsios and Pomoni-Papaioannou, 1998), and several features indicate the pre-existence of evaporites, whereas alternations of dolomites and evaporites comprise a very common association in the subsurface (IGRS-IFP, 1966; BP, 1971). We suggest that, the shale fragments, with significant content in organic matter, included within the Triassic breccias were initially deposited as stratigraphic layers in relatively shallow restricted sub-basins inside the evaporitic basin. The lack of detailed stratigraphy of evaporitic sequence in Ionian Zone does not allow any suggestion about the exact stratigraphic position of the shale layers; consequently, it is not possible to correlate the deposition of these layers with any geological event of Triassic age (e.g., sea level changes, local subsidence, anoxic events etc.). However, the establishment of the

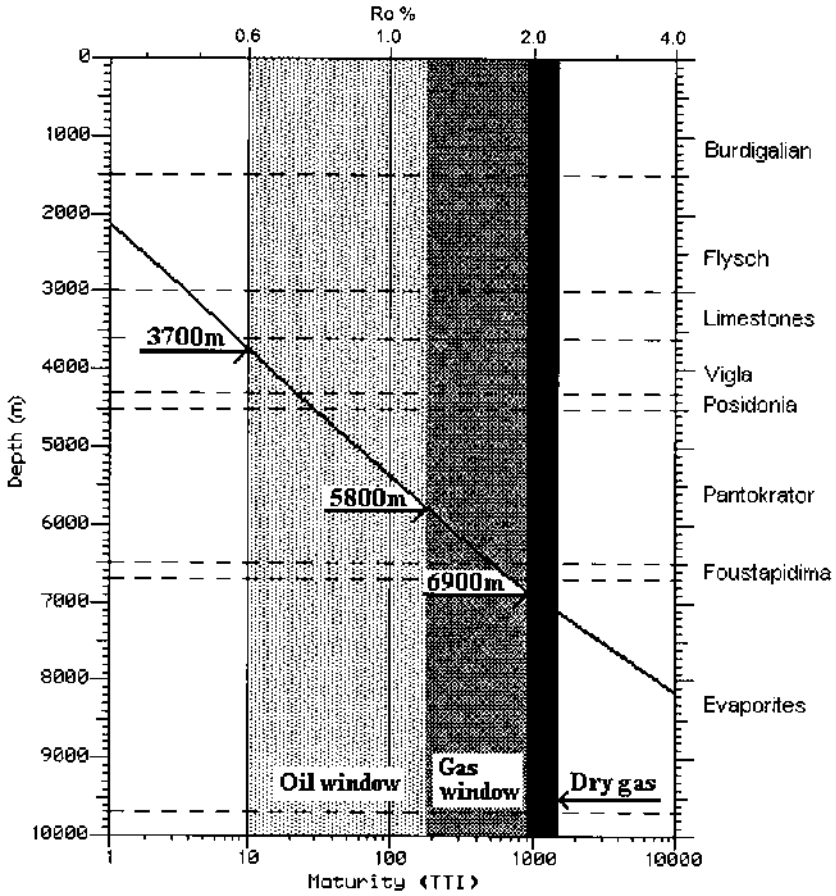

Fig. 12. Time temperature index (TTI) increased by depth, in Botsara sub-basin.

evaporitic sedimentation in the entire basin favored the preservation of the organic matter (Powell, 1986; Miller, 1990). Consequently, the processes that formed the evaporite dissolution collapse breccias caused also the fragmentation of the initially organic rich shale layers, which are present actually as organic rich shale fragments in the Triassic breccias.

8. Conclusions

(1) Five horizons of possible source rocks have been identified in the Ionian Zone of northwestern Greece: the Vigla shales (Cenomanian-Turonian), the Upper Posidonia Beds (Callovian-Tithonian), the Lower Posidonia Beds (Toarcian-Aalenian), the marls at the base of the Ammonitico Rosso (Lower Toarcian) and some Triassic breccia horizons containing shale fragments. All the above source-rocks horizons have good hydrocarbon potential and their organic matter is of type I–II.

(2) In the deeper areas of the Botsara sub-basin the oil window is located in the 3700–5800 m interval. Consequently, the Triassic shales have already entered the gas window. The Lower and Upper Posidonia Beds and the marls at the base of the Ammonitico Rosso are mature in terms of oil generation. The maturity level of the Vigla Shales corresponds to the early maturation stage. As far as the timing of maturation of the principal oil-source horizons is concerned, the Triassic shale horizons entered the oil window in the Late Jurassic, while the Lower Peosidonia Beds entered it in the Serravalian.

(3) The preservation of the organic matter in the Lower and Upper Posidonia Beds through Toarcian to Tithonian, and in the marls at the base of the Ammonitico Rosso during Early Toarcian times, is directly related to the geometry of the syn-rift period of the Ionian Basin. Organic matter preservation in the Vigla Shales is related to the sub-basins that were preserved by the continuation of halokinetic movements during the post rift period. Thus anoxic conditions were selectively created during the whole syn-rift and sometimes preserved during the post-rift period. The geometry of the restricted sub-basins favored water stagnation and consequently the development of locally euxinic conditions in the bottom waters. This particular geometry of the syn-rift and

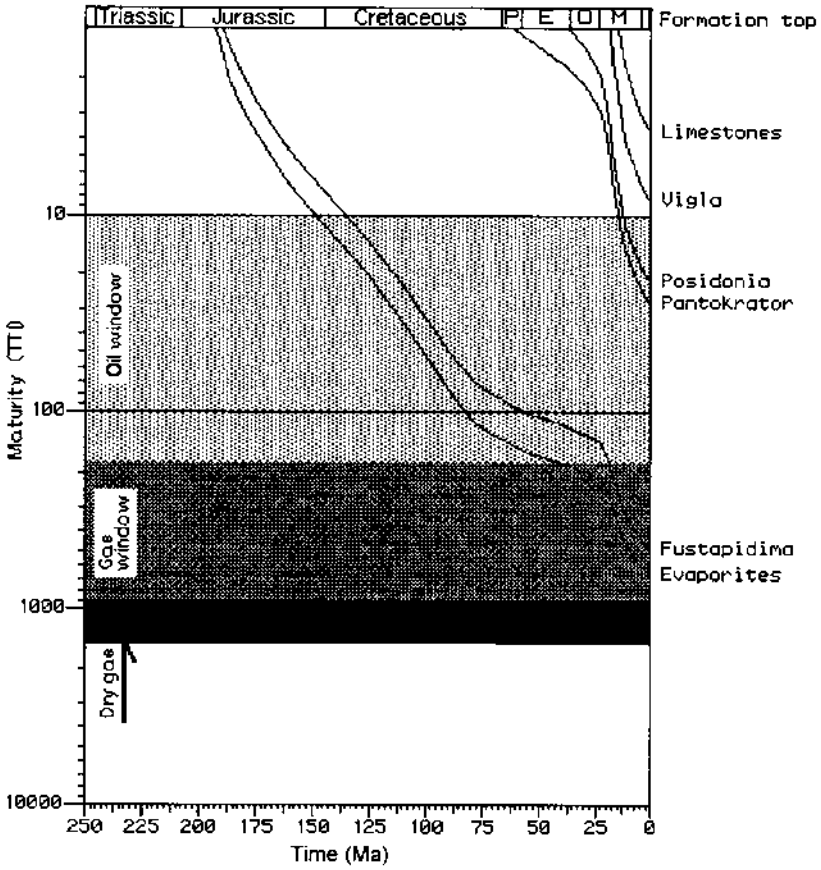

Fig. 13. Maturity through time, indicating the time that the possible source rocks entered the oil generation window in Botsara sub-basin.

post-rift period of the Ionian Zone promoted the anoxic events that are also reported from the Tethys ocean during Early Toarcian and Cenomanian/Turonian times. The organic rich shale fragments within the Triassic breccias were initially deposited as stratigraphic layers in relatively shallow restricted sub-basins inside the evaporitic basin. The establishment of evaporitic sedimentation in the entire basin favored the preservation of the organic matter. The processes accounting for the formation of the evaporite dissolution collapse breccias caused also the fragmentation of the initial organic rich layers, which presently occur as organic rich shale fragments incorporated within the Triassic breccias.

Appendix

Rock Eval pyrolysis data. For identification of parameters see Fig. 6.

Depth	T_{max}	S1	S2	S3	PI	S2/S3	PC	TOC	PP	HI	OI
Ioannina-1 well											
Vigla shales											
460	418	0.24	8.28	0.17	0.03	48.70	0.71	1.62	8.52	511	10
465	418	0.25	11.56	0.24	0.02	48.16	0.98	2.07	11.81	558	11
470	417	0.11	7.62	0.25	0.01	30.48	0.64	1.51	7.73	504	16
475	416	0.20	13.38	0.30	0.01	44.60	1.13	2.24	13.58	597	13
480	423	0.19	7.20	0.29	0.03	24.82	0.61	1.51	7.39	476	19
485	417	0.13	7.16	0.29	0.02	24.68	0.60	1.44	7.29	497	20

continued

Depth	T_{max}	S1	S2	S3	PI	S2/S3	PC	TOC	PP	HI	OI
Posidonia beds											
615	422	0.22	10.23	0.30	0.02	34.10	0.87	1.79	10.45	571	16
620	422	0.10	5.70	0.19	0.02	30.00	0.48	1.05	5.80	542	18
625	422	0.24	9.27	0.41	0.03	22.60	0.79	2.00	9.51	463	20
630	419	0.13	7.67	0.23	0.02	33.34	0.65	1.48	7.80	518	15
635	423	0.17	8.35	0.21	0.02	39.76	0.71	1.55	8.52	538	13
640	423	0.16	8.14	0.24	0.02	33.91	0.69	1.55	8.30	525	15
645	426	0.14	6.59	0.27	0.02	24.40	0.56	1.30	6.73	506	20
655	425	0.23	8.62	0.22	0.03	39.18	0.73	1.59	8.85	542	13
675	429	0.15	6.16	0.22	0.02	28.00	0.52	1.21	6.31	509	18
680	416	0.21	6.58	0.22	0.03	29.90	0.56	1.40	6.79	470	15
685	419	0.14	8.26	0.23	0.02	35.91	0.70	1.66	8.40	497	13
690	421	0.18	7.64	0.24	0.02	31.83	0.65	1.60	7.82	477	15
695	421	0.17	8.96	0.26	0.02	34.46	0.76	1.64	9.13	546	15
715	411	0.16	3.92	0.14	0.04	28.00	0.34	0.62	4.08	632	22
725	421	0.17	7.83	0.27	0.02	29.00	0.66	1.50	8.00	522	18
730	416	0.43	5.02	0.17	0.08	29.52	0.45	0.91	5.45	552	19
755	423	0.12	6.40	0.26	0.02	24.61	0.54	1.39	6.52	460	18
800	422	0.14	4.23	0.31	0.03	13.64	0.36	1.08	4.37	391	28
805	422	0.08	3.92	0.20	0.02	19.60	0.33	0.91	4.00	430	21
820	419	0.20	10.51	0.28	0.02	37.53	0.89	1.94	10.71	541	14
830	420	0.28	14.17	0.34	0.02	41.67	1.20	2.54	14.45	557	13
840	422	0.19	8.53	0.25	0.02	34.12	0.72	1.60	8.72	533	15
850	428	0.21	7.22	0.17	0.03	42.47	0.61	1.38	7.43	523	12
865	431	0.23	9.06	0.18	0.02	50.33	0.77	1.64	9.29	552	10
870	428	0.15	6.68	0.15	0.02	44.53	0.56	1.12	6.83	596	13
895	429	0.61	14.16	0.22	0.04	64.36	1.23	2.56	14.77	553	8
900	431	0.53	11.04	0.16	0.05	69.00	0.96	1.74	11.57	634	9
910	433	0.69	33.19	0.25	0.02	132.76	2.82	5.87	33.88	565	4
920	432	0.58	20.96	0.19	0.03	110.31	1.79	3.46	21.54	605	5
940	430	0.68	63.41	0.24	0.01	264.20	5.34	9.82	64.09	645	2
945	431	0.23	28.67	0.17	0.01	168.64	2.40	4.50	28.90	637	3
964	416	0.87	14.51	0.25	0.06	58.04	1.28	2.75	15.38	527	9
970	429	0.12	12.75	0.22	0.01	57.95	1.07	1.88	12.87	678	11
1005	432	0.31	11.60	0.27	0.03	42.96	0.99	1.69	11.91	686	15
1010	421	0.15	5.00	0.17	0.03	29.41	0.42	0.96	5.15	520	17
Triassic breccias											
1250	436	0.88	73.14	0.66	0.01	110.81	6.16	11.15	74.02	655	5
1255	430	0.71	98.08	0.74	0.01	132.54	8.23	16.12	98.79	608	4
1260	429	0.34	23.70	0.24	0.01	98.75	2.00	3.84	24.04	617	6
1265	429	0.50	44.78	0.37	0.01	121.02	3.77	7.69	45.28	582	4
1270	421	0.53	8.33	0.21	0.06	39.66	0.73	1.62	8.86	514	12
1275	428	0.07	1.44	0.18	0.05	8.00	0.12	0.31	1.51	464	58
1380	429	0.02	0.18	0.11	0.10	1.63	0.01	0.06	0.20	300	183
1400	428	0.13	2.25	0.26	0.05	8.65	0.19	0.57	2.38	394	45
1450	428	0.15	3.16	0.22	0.05	14.36	0.27	0.65	3.31	486	33
1520	424	0.10	2.55	0.18	0.04	14.16	0.22	0.51	2.65	500	35
Dragopsa-1 well, undifferentiated Posidonia beds											
1479	415	0.14	3.65	0.40	0.04	9.13	0.31	1.01	3.79	361	40
1481	415	1.67	48.47	1.33	0.03	36.44	4.17	8.52	50.14	569	16
1483	416	3.54	91.88	2.30	0.04	39.95	7.95	14.90	95.42	617	15
1485.1	418	4.51	45.70	1.09	0.09	41.93	4.18	7.56	50.21	604	14
1485.2	415	7.78	76.51	2.22	0.09	34.46	7.02	12.73	84.29	601	17
1485.3	414	8.56	65.62	2.84	0.12	23.11	6.18	11.59	74.18	566	25
1485.4	415	3.89	112.96	3.63	0.03	31.12	9.73	19.12	116.85	591	19
1485.7	416	0.59	6.25	0.75	0.09	8.33	0.57	0.98	6.84	638	77
1485.8	415	1.90	25.85	1.55	0.07	16.68	2.31	3.87	27.75	668	40
1485.9	415	1.05	9.41	0.77	0.10	12.22	0.87	1.49	10.46	632	52
1486	415	5.35	57.45	1.52	0.09	37.80	5.23	9.50	62.80	605	16
1487	419	7.05	97.32	4.70	0.07	20.71	8.69	15.24	104.37	639	31

continued

Depth	T_{max}	S1	S2	S3	PI	S2/S3	PC	TOC	PP	HI	OI
1489	416	3.99	121.85	5.04	0.03	24.18	10.48	18.18	125.84	670	28
1501	418	1.10	24.71	1.30	0.04	19.01	2.15	4.09	25.81	604	32
1503	419	0.98	47.49	3.23	0.02	14.70	4.03	8.02	48.47	592	40
1505	416	1.81	56.49	2.37	0.03	23.84	4.85	9.44	58.30	598	25
1507	415	1.91	31.64	1.42	0.06	22.28	2.79	5.55	33.55	570	26
1509	415	2.97	72.65	3.87	0.04	18.77	6.30	12.72	75.62	571	30
1511	417	1.45	47.88	3.08	0.03	15.55	4.11	8.05	49.33	595	38
1513	416	2.54	102.08	4.12	0.02	24.78	8.71	17.20	104.62	593	24
1515	414	1.31	44.49	4.10	0.03	10.85	3.81	6.85	45.80	649	60
1517	416	3.41	80.57	2.71	0.04	29.73	6.99	13.49	83.98	597	20
1519	415	1.61	62.68	2.91	0.03	21.54	5.33	11.68	64.29	537	25
1521	416	2.70	79.18	1.95	0.03	40.61	6.82	13.55	81.88	584	14
1523	417	4.74	77.78	3.55	0.06	21.91	6.87	13.22	82.52	588	27
1525	412	3.31	94.30	4.53	0.03	20.82	8.13	15.45	97.61	610	29
1527	417	2.03	88.90	3.16	0.02	28.13	7.57	15.01	90.93	592	21
1529	411	1.93	67.29	2.42	0.03	27.81	5.76	8.93	69.22	754	27
1531	414	0.51	14.66	1.02	0.03	14.37	1.26	2.67	15.17	549	38
1533	413	0.31	11.14	1.46	0.03	7.63	0.95	2.00	11.45	557	73
1535	415	1.45	37.59	1.25	0.04	30.07	3.25	3.24	39.04	1160	39
1537	416	0.31	6.55	0.67	0.05	9.78	0.57	1.07	6.86	612	63
1539	415	2.16	98.20	3.10	0.02	31.68	8.36	16.21	100.36	606	19
1541	414	1.47	64.80	2.55	0.02	25.41	5.52	10.34	66.27	627	25
1543	416	1.90	85.96	3.09	0.02	27.82	7.32	15.04	87.86	572	21
1545	414	1.91	76.70	2.37	0.02	32.36	6.55	12.98	78.61	591	18
1547	415	4.55	95.39	3.03	0.05	31.48	8.32	16.77	99.94	569	18
1549	413	0.35	14.27	0.91	0.02	15.68	1.21	2.22	14.62	643	41
1551	413	0.75	34.55	1.20	0.02	28.79	2.94	5.37	35.30	643	22
1553	415	0.51	11.16	0.85	0.04	13.13	0.97	1.85	11.67	603	46
1555	414	0.81	30.63	1.03	0.03	29.74	2.62	5.68	31.44	539	18
1557	417	1.13	49.50	3.34	0.02	14.82	4.21	7.96	50.63	622	42
1559	414	2.62	50.00	3.24	0.05	15.43	4.38	8.50	52.62	588	38
1561	416	2.79	75.00	1.91	0.04	39.27	6.48	13.36	77.79	561	14
1563	415	0.21	23.13	2.91	0.01	7.95	1.94	3.59	23.34	644	81
1565	417	0.36	13.88	0.92	0.03	15.09	1.18	1.92	14.24	723	48
1567	415	0.26	10.23	0.92	0.02	11.12	0.87	1.42	10.49	720	65
1571	415	0.23	10.25	1.11	0.02	9.23	0.87	1.74	10.48	589	64
1573	413	1.55	73.86	2.87	0.02	25.74	6.28	11.99	75.41	616	24
1575	411	0.17	11.24	0.89	0.01	12.63	0.95	1.49	11.41	754	60
1577	416	0.67	20.91	1.17	0.03	17.87	1.79	3.44	21.58	608	34
1579	415	0.32	9.79	0.85	0.03	11.52	0.84	1.75	10.11	559	49
1581	417	0.24	14.54	1.20	0.02	12.12	1.23	2.65	14.78	549	45
1583	420	1.20	25.18	1.72	0.05	14.64	2.19	4.03	26.38	625	43
1585	416	2.90	116.29	3.83	0.02	30.36	9.93	20.06	119.19	580	19
1587	415	2.01	61.49	3.41	0.03	18.03	5.29	10.00	63.50	615	34
1589	410	0.24	7.13	0.30	0.03	23.76	0.61	1.43	7.37	498	20
1591	412	0.48	11.97	0.33	0.04	36.27	1.03	2.11	12.45	567	15
1593	411	0.15	5.47	0.29	0.03	18.86	0.46	1.14	5.62	479	25
1595	410	0.16	4.98	0.32	0.03	15.56	0.42	1.06	5.14	469	30
1597	412	0.22	4.61	0.35	0.05	13.17	0.40	0.96	4.83	480	36
1599	413	0.23	5.62	0.33	0.04	17.03	0.48	1.23	5.85	456	26

Sample	T_{max}	S1	S2	S3	PI	S2/S3	PC	TOC	PP	HI	OI
Mavronoros, Upper Posidonia beds											
2407	425	0.12	4.60	1.20	0.03	3.83	0.39	2.51	4.72	183	47
2408	412	0.23	14.28	0.76	0.02	18.78	1.20	3.47	14.51	411	21
Gotzikas, Vigla shales											
1402	411	13.27	165.32	21.15	0.07	7.82	14.88	21.61	178.59	765	98
1403	420	8.46	174.11	3.93	0.05	44.30	15.21	19.10	182.57	912	21
1410	423	0.18	4.67	1.07	0.04	4.36	0.40	0.94	4.85	497	114
1412	423	0.22	9.30	0.88	0.02	10.57	0.79	1.82	9.52	511	48

continued

Depth	T_{max}	S1	S2	S3	PI	S2/S3	PC	TOC	PP	HI	OI
1413	422	0.28	11.41	0.66	0.02	17.29	0.97	1.83	11.69	623	36
1414	419	0.20	8.39	1.06	0.02	7.92	0.71	1.50	8.59	559	71
1415	424	0.19	7.99	1.07	0.02	7.47	0.68	1.56	8.18	512	69
1416	421	0.20	9.58	1.55	0.02	6.18	0.81	2.54	9.78	377	61
Paliogrimpiani, undifferentiated Posidonia beds											
2078	432	0.03	1.70	0.45	0.02	3.77	0.14	0.88	1.73	193	51
2079	0	0.01	0.00	0.30	0.00	0.00	0.00	0.11	0.01	0	272
2083	0	0.02	0.00	0.06	1.00	0.00	0.00	0.11	0.02	0	54
2084	0	0.01	0.00	0.63	0.00	0.00	0.00	0.18	0.01	0	350
2085	0	0.01	0.00	0.24	0.00	0.00	0.00	0.12	0.01	0	200
2086	0	0.01	0.01	0.50	0.50	0.02	0.00	0.21	0.02	4	238
2087	402	0.01	0.10	0.78	0.10	0.12	0.00	0.27	0.11	37	288
2089	0	0.01	0.00	0.05	0.00	0.00	0.00	0.09	0.01	0	55
2091	0	0.00	0.03	0.30	0.00	0.10	0.00	0.16	0.03	18	187
2092	0	0.01	0.04	0.23	0.25	0.17	0.00	0.18	0.05	22	127
Toka, Ammonitico Rosso base											
2434	426	0.03	0.08	0.10	0.30	0.80	0.00	0.11	0.11	72	90
2435	425	0.02	0.13	0.05	0.14	2.60	0.01	0.14	0.15	92	35
2437	427	0.01	1.23	0.23	0.01	5.34	0.10	0.93	1.24	132	24
2438	428	0.00	0.07	0.09	0.00	0.77	0.00	0.14	0.07	50	64
2439	429	0.06	0.91	0.12	0.06	7.58	0.08	0.77	0.97	118	15
2440	422	0.13	17.41	0.51	0.01	34.13	1.46	4.07	17.54	427	12
2441	422	0.11	17.54	0.43	0.01	40.79	1.47	3.46	17.65	506	12
2442	430	0.06	2.89	0.18	0.02	16.05	0.24	1.45	2.95	199	12
2443	423	0.08	0.14	0.20	0.36	0.70	0.01	0.45	0.22	31	44
North Mavroudi, Triassic shale fragments											
281	452	0.38	0.67	0.46	0.36	1.46	0.08	1.25	1.05	54	37
282	455	0.07	0.21	0.33	0.25	0.64	0.02	0.64	0.28	33	52
283	449	0.15	0.18	0.34	0.45	0.53	0.02	0.59	0.33	31	58
284	452	0.52	0.78	0.53	0.40	1.47	0.10	1.29	1.30	60	41
Elataria, Lower Posidonia beds											
927	420	0.04	6.17	0.76	0.01	8.12	0.54	1.62	6.21	381	47
928	419	0.08	5.53	0.86	0.01	6.43	0.49	1.32	5.61	419	65
929	421	0.07	4.36	0.61	0.02	7.15	0.38	1.10	4.43	396	55
930	406	0.25	6.51	0.53	0.04	12.28	0.58	1.15	6.76	566	46
933	423	0.10	5.04	0.64	0.02	7.88	0.44	1.10	5.14	458	58
934	419	0.15	6.94	0.71	0.02	9.77	0.61	1.38	7.09	503	51
935	420	0.11	4.52	0.51	0.02	8.86	0.40	0.98	4.63	461	52
936	422	0.12	10.40	0.96	0.01	10.83	0.90	2.02	10.52	515	48
937	421	0.09	5.54	0.76	0.02	7.29	0.49	1.20	5.63	462	63
938	415	0.17	10.84	0.81	0.02	13.38	0.94	1.80	11.01	602	45
939	416	0.10	6.31	0.84	0.02	7.51	0.55	1.07	6.41	590	79
940	415	0.11	6.84	0.82	0.02	8.34	0.60	1.52	6.95	450	54
941	419	0.16	8.45	0.52	0.02	16.25	0.73	1.57	8.61	538	33
943	422	0.20	9.25	0.77	0.02	12.01	0.81	1.37	9.45	675	56
945	418	0.15	7.64	0.77	0.02	9.92	0.67	1.22	7.79	626	63
946	415	0.23	10.07	0.78	0.02	12.91	0.88	1.47	10.30	685	53
947	418	0.35	17.49	0.68	0.02	25.72	1.50	2.32	17.84	754	29
948	420	0.24	8.34	0.51	0.03	16.35	0.73	1.35	8.58	618	38
949	414	0.20	6.29	0.80	0.03	7.86	0.56	0.97	6.49	648	82
950	413	0.11	5.86	0.57	0.02	10.28	0.51	0.87	5.97	674	66

Acknowledgements

We thank J. G. Palacas for useful discussions, H. C. Jenkyns, an anonymous reviewer for their helpful reviews, and D. G. Roberts for his helpful comments. We are very grateful to the Hellenic Petroleum S.A. (Exploration and Production Division) for performing the analytical work.

References

Aubouin, J. (1959). Contribution à l'étude géologique de la Grèce septentrionale: les confins de l'Epire et de la Thessalie: *Ann. géol. Pays Hell*., *1*(IX), 1–483.

Baldanza, A., & Mattioli, E. (1992). Biostratigraphical synthesis of nannofossils in the early Middle Jurassic of southern Tethys. In B. Hamrsmid & J. Young (eds), *Proceedings of the Fourth International Nannoplankton Association Conference* (pp. 111–141). Prague 1991, *Knihovnicka Zemniho Plynu a Nafty*. 14a.

Baudin, F., & Lachkar, G. (1990). Géochimie organique et palynologie du Lias supérieur en zone ionienne (Grèce). Exemple d'une sédimentation anoxique conservée dans une paléo-marge en distension. *Bull. Soc. géol. France*, *8*(VI; 1) 123–132.

Bernoulli, D., & Renz, O. (1970). Jurassic Carbonate Facies and New Ammonite Faunas from Western Greece. *Eclogae Geol. Helv*., *63*(2), 573–607.

Bertrand, Ph., Bordenave, M. L., Brosse, E., Espitalie, J., Houzay, J. P., Pradier, B., Vandenbroucke, M., & Walgenwitz, F. (1993). Other methods and tools for source rocks appraisal. In M. L. Bordenave (Ed.), *Applied Petroleum Geochemistry* (pp. 279–371). Paris: Technip.

Bizon, G. (1967). Contribution à la connaissance des foraminifères planctoniques d'Epire et des îles ioniennes (Grèce occidentale) depuis le Paléogène supérieur jusqu'au Pliocène, Paris: Editions Technip, 1–144.

Bordenave, M. L., Espitalie, J., Leplat, P., Oudin, J. O., & Vandenbroucke, M. (1993). Screening techniques for source rocks evaluation. In M. L. Bordenave (ed.), *Applied Petroleum Geochemistry* (p. 217–278). Paris: Technip.

BP (British Petroleum Company Limited) (1971). The geological results of petroleum exploration in western Greece: *Inst. geol. subs. Res*., Athens, *10*, 1–73.

Claypool, G. E., Love, A. H., & Maughan, E. K. (1978). Organic geochemistry, incipient metamorphism, and oil generation in black shales members of Phosphoria formation, Western Interior United States. *AAPG Bulletin*, *62*, 98–120.

Dragastan, O., Papanikos, D., & Papanikos, P. (1985). Foraminifères, Algues et microproblematica du Trias de Messopotamos, Epire (Grèce continentale). *Rev. Micropaleont*., *27*(4), 244–248.

Espitalie, J., Laporte, J. L., Madec, M., Marquis, F., Leplat, P., Paulet, J., & Boutefeu, A. (1977). Methode rapide de caracterisation des roches meres de leur potentiel petrolier et de leur degre d'evolution. *Rev. Inst. Franc. du Petr*., *v. XXXII*, 23–42.

Farrimond, P., Eglinton, G., Brassell, S. C., & Jenkyns, H. C. (1989). Toarcian anoxic event in Europe: An organic geochemical study. *Marine and Petroleum Geology*, *6*, 136–147.

Farrimond, P., Eglinton, G., Brassell, S. C., & Jenkins, H. C. (1990). The Cenomanian/Turonian anoxic event in Europe. An organic geochemical study. *Marine and Petroleim Geology*, *7*, 75–89.

Fertl, W. H. (1983). Gamma ray spectral logging: A new evaluation frontier. *World Oil* May, 147–155.

IGRS-IFP (Institut de Géologie et Recherches du Sous-sol—Institut Français du Petrole) (1996). Etude géologique de l'Epire (Grèce nord-occidentale): Paris: Ed. Technip, 306.

Jenkyns, H. C. (1988). The Early Toarcian (Jurassic) anoxic event: Stratigraphic, sedimentary, and geochemical evidence. *Am. J. Sci*., *288*, 101–151.

Karakitsios, V. (1988). Sur la différenciation de la zone ionienne en Epire (Grèce Nord-occidentale). Proc. 3rd Geol. Congress, Athens, 1986: *Bull. Geol. Soc. Greece*, *20/2*, 181–196.

Karakitsios, V. (1990). Chronologie et géometrie de l'ouverture d'un bassin et de son inversion tectonique: le bassin ionien (Epire, Grèce): (Th. Doct. Univ. Paris IV). *Mem. Sc. Terre Univ. P: et M. Curie*, Paris, *91–4*, 310.

Karakitsios, V. (1992). Ouverture et inversion tectonique du basin ionien (Epire, Grece). *Ann. Geol. Pays Hellen*, *35*, 85–318.

Karakitsios, V. (1995). The influence of preexisting structure and halokinesis on organic matter preservation and thrust system evolution in the Ionian basin, Northwestern Greece. *AAPG Bulletin*, *79*, 960–980.

Karakitsios, V., & Tsaila-Monopolis, S. (1988). Données nouvelles sur les niveaux supérieurs (Lias inférieur-moyen) des Calcaires de Pantokrator (zone ionienne moyenne, Epire, Grèce continentale). Description des Calcaires de Louros. *Rev. Micropaleont*., *31*(1), 49–55.

Karakitsios, V., Danelian, T., & De Wever, P. (1988). Datation par les radiolaires des Calcaires à Filaments, Schists à Posidonies supérieurs et Calcaires de Vigla (zone ionienne, Epire, Grèce) du Callovient au Tithonique terminal. *Compte Rendu de l'Académie des Sciences*, *306*(II), 367–372.

Karakitsios, V., & Tsaila-Monopolis, S. (1990). Données nouvelles sur les niveaux inférieurs (Trias supérieur) de la serie calcaire ionienne en Epire (Grèce continentale). Conséquences stratigraphiques. *Rev. Paleobiol*., *9*(1), 139–147.

Karakitsios, V., & Koletti, L. (1992). Critical revision of the age of the basal Vigla Limestones (Ionian zone, Western Greece), based on Nannoplankton and Calpionellids, with Paleogeographical consequences. In (Eds.) B. Hamrsmid and J. Young, *Proceedings of the Fourth International Nannoplankton Association Conference* (pp. 165–177) Prague, 1991, *Knihovnicka Zemniho Plynu a Nafty*. 14a.

Karakitsios, V., & Rigakis, N. (1996). New oil source rocks cut in Greek Ionian basin. *Oil & Gas Journal*, *94*(7), 56–59.

Karakitsios, V., & Pomoni-Papaioannou, F. (1998). Brecciation patterns of the Triassic solution-collapse breccias of the Ionian zone (western Greece): evidence for early diagenetic calichification. In J. C. Canaveras, M. Angeles Garcia del Cura, J. Soris, (Eds.), *15th International Sedimentological Congress*, *Alicante* 1998 (pp. 461–462), Spain.

Koukouzas, K., Grigoris, P., Papstavrou, S., Galanos, D., & Manolarakis, S. (1978). Report on the preliminary investigation of phosphoric-uranium outcrops and radioactive anomalies of Epirus-Ioannina regions. *Inst. geol. Miner. Exploration of Greece* (Internal report).

Mackenzie, A. S. (1984). Applications of biological markers in petroleum geochemistry. *Advances in Org. Geochem*., *1*, 115–214.

Mello, M. R., Gaglianone, P. C., Brassell, S. C., & Maxwell, J. R. (1988). Geochemical and biological marker assessment of depositional environments using Brazilian offshore oils. *Marine and petroleum Geology*, *5*, 205–223.

Miller, R. G. (1990). A paleoceanographic approach to the Kimmeridge clay formation. In A. Y. Huc (Ed.), *Deposition of Organic Facies* (pp. 13–26). AAPG Studies in Geology, 30.

Nikolaou, C. A. (1986). *Contribution to the knowledge of the Neogene, the geology and the Ionian and pre-Apulian zone limits in relation to the petroleum geology observations in Strophades, Zakynthos and Kephallinia islands*. p. 228. Th. Doct. Univ. Athens.

Palacas, J. G., Anders, D. E., & King, J. D. (1984). South Florida basin—A prime example of Carbonate source rocks of petroleum. In J. G. Palacas (Ed.), *Petroleum geochemistry and source rock potential of Carbonates rocks* (pp. 71–96). AAPG, Studies in Geology 18.

Palacas, J. G., Monopolis, D., Nicolaou, C. A., & Anders, D. E. (1986). Geochemical correlation of surface and subsurface oils, Western Greece. In D. Laythaeuser and J. Rullkötter (Eds.), *Advances in organic geochemistry* 1985 (pp. 417–423). Org. Geochem., 10.

Palacas, G. J., Anders, D. E., King, J. D., & Lubeck, C. M. (1988). Use of biological markers in determining thermal maturity of biodegraded heavy oils and solid bitumens. In R. F. Meyer and E. J. Wiggins (Eds.), *Proceedings of the fourth UNITAR/UNDP Intern. Conf. on heavy crude and tar sands*: *Alberta oil sands technology and research authority* (pp. 575–631). Edmonton, Alberta, Canada 2.

Peters, K. E. (1986). Guidelines for evaluating petroleum source rock using programmed pyrolysis. *AAPG Bulletin*, *70*, 318–329.

Peters, K. E., & Moldowan, J. M. (1993). *The biomarker guide*: *Interpreting molecular fossils in petroleum and ancient sediments*. New Jersey: Prentice Hall (eds), p. 1–363.

Pomoni-Papaioannou, F., & Tsaila-Monopolis, S. (1983). Petrographical, Sedimentological and Micropaleontological studies in an evaporite outcrop, West of Ziros lake (Epirus-Greece). *Riv. Ital. Paleont. Strat*., Milano, *88*(3), 387–400.

Powell, T. G. (1986). Petroleum geochemistry and depositional setting of lacustrine source rocks. *Marine and petroleum geology*, *3*, 200–219.

Renz, C. (1955). Die vorneogene Stratigraphie der normal-sedimentären Formationen Griechenlands: *Inst. Geol. Subsurf. Res*, Athens, 637.

Roussos, N., & Marnelis, F. (1995). Greece licensing round to focus on western sedimentary basins. *Oils & Gas Journal*, *93*(10), 58–62.

Schmoker, J. W. (1981). Determination of organic-matter content of Appalachian Devonian shales from gamma-ray logs. *AAPG Bulletin*, *65*, 1285–1298.

Teichmuller, M. (1986). Organic petrology of source rocks, history and state of the art. In D. Leythaeuser & J. Rullkötter (Eds.), *Advances in organic geochemistry* 1985, (pp.581–599), *Org. Geochem* v. 10.

Tissot, B. P. (1984). Recent advances in petroleum geochemistry applied to hydrocarbon exploration. *AAPG Bulletin*, *68*, 545–563.

Tissot, B. P., & Welte, D. H. (1984). Petroleum formation and occurrence. Berlin: Springer-Verlag (eds), p. 1–699.

Walzebuck, J. P. (1982). Bedding types of the Toarcian black shales in NW-Greece. In G. Einsel & A. Seilacher (Eds.) *Cyclic and event stratification* (pp. 512–525). New York: Springer-Verlag.

Waples, D. W. (1980). Time and temperature in petroleum formation: Application of Lopatin's method to petroleum exploration. *AAPG Bulletin*, *64*, 916–926.